universität wien

MASTERARBEIT / MASTER'S THESIS

Titel der Masterarbeit / Title of the Master's Thesis

„Pre-clinical evaluation of the binding properties of potential muscarinic acetylcholine receptor ligands“

verfasst von / submitted by

Katharina Pacher, BSc

angestrebter akademischer Grad / in partial fulfilment of the requirements for the degree of

Master of Science (MSc)

Wien, 2019/ Vienna 2019

Studienkennzahl lt. Studienblatt / degree programme code as it appears on the student record sheet:	A 066 862
Studienrichtung lt. Studienblatt / degree programme as it appears on the student record sheet:	Masterstudium Chemie
Betreut von / Supervisor:	Assoz. Prof. Mag. Dr. Wolfgang Wadsak, Privatdoz.

Acknowledgement

Throughout the course of my master's thesis I have received a great deal of support and I would like to use this opportunity to thank everyone who assisted me.

First of all, I want to thank my supervisor Assoc.-Prof. Mag. Dr. Wolfgang Wadsak for the opportunity to work at the nuclear medicine department at the Vienna General Hospital and doing research in such a growing and interesting field.

I am particularly grateful for my co-supervisors.
Dr. Verena Pichler, for always taking time to help me out, when I had a question or ran into any kind of difficulty.
Marius Ozenil, MSc., for having an endless amount of patience in explaining different techniques and equipment, as well as always being there when I needed advice.
Without their guidance and persistent help this thesis would not have been possible.

The encouragement and support, as well as the light-hearted conversations with everyone in the nuclear medicine team (Verena, Marius, Chrysoula, Neydher, Eva, Karsten, Sarah, Theresa, …) were invaluable to me.

I would also like to thank the other students (Lukas, Julia and Tina), who worked on their theses at the same time as me, for all the fun we had and for their help, whenever I needed it.

Last but not least, I would like to thank my family and friends for their unfailing support and continuous encouragement during all of my studies.

Thank you!

Abstract

The muscarinic acetylcholine receptors (mAChRs) are a family of G-protein-coupled receptors and are found mainly in the central nervous system. They play an important role in neuronal functions and are an interesting target in a variety of neurodegenerative diseases, like Parkinson's or Alzheimer's dementia. Even though, there are some already established tracers for positron emission tomography (PET) imaging of mAChRs, there is still the need to improve them, mostly in regard to subtype selectivity. Within this thesis the binding properties of novel potential ligands for this receptor are analysed and evaluated for their structure-activity relationships. The ligands are derivatives of the natural ligand arecoline, which is found in the betel nut. In the beginning the derivatives of arecoline were tested for their affinity using a competitive radioligand binding assay with the filtration method. The K_i was calculated using the Cheng-Prussoff-equation. In the next step the interaction with the off-target acetylcholinesterase was analysed. Therefore, two different experiments were set up, to determine if the arecoline derivatives were an inhibitor or a substrate for the acetylcholinesterase. From these experiments four structures with promising K_i values against the muscarinic acetylcholine receptors but with no interaction to the off target acetylcholinesterase, were identified. In the end, the binding kinetics of the compounds with the highest affinity were studied using a LigandTracer®. These experiments showed contradictory results. Consequently, the set up of the experiment was examined in order to analyse if the results occur from unspecific binding, accumulation of the tracer or other effects. However, further experiments should be used to establish a new set up for the LigandTracer® experiment. Apart from that, different, less lipophilic structures will be tested for their binding affinities to overcome unspecific binding of the here investigated substances.

Kurzfassung

Die muskarinischen Acetylcholinrezeptoren (mAChR) gehören zur Familie der G-Protein-gekoppelten Rezeptoren und befinden sich hauptsächlich im zentralen Nervensystem. Die mAChR spielen eine wichtige Rolle in verschiedenen neuronalen Funktionen und stellen deswegen ein interessantes Target in neurodegenerative Krankheiten, wie Alzheimer oder Parkinson, dar. Obwohl es bereits etablierte Tracer für die Bildgebung mittels Positronen-Emissions-Tomographie (PET) gibt, sind diese noch verbesserungswürdig, vor allem im Bereich der Subtypenselektivität. Diese Masterarbeit beschäftigt sich mit den Bindungseigenschaften neuer möglicher Liganden für eben diese Rezeptoren. Die verwendeten Liganden sind Derivate des natürlich vorkommenden Liganden Arecolin, welcher in der Betelnuss vorkommt. Zu Beginn wurde die Affinität der Arecolin-Derivate mit Hilfe eines kompetitiven Radioligandenbindungsassays mit Hilfe der Filtrationsmethode bestimmt. Der K_i-Wert wurde anschließend über die Cheng-Prussoff-Gleichung berechnet. Im nächsten Schritt wurden die Interaktionen der Arecolin-Derivate mit dem unerwünschten Target Acetylcholinesterase analysiert. Hierfür wurden zwei unterschiedliche Experimente durchgeführt, um festzustellen ob die Arecolin-Derivate als Substrat oder als Inhibitor der Acetylcholinesterase fungieren. Aus diesen Experimenten gingen vier Strukturen mit vielversprechenden Bindungseigenschaften zum mAChR hervor, die überdies keine Interaktionen mit der strukturell verwandten Acetylcholinesterase zeigten. Zum Schluss wurde die Bindungskinetik der besten Verbindungen mittels LigandTracer® Technologie analysiert. Die Experimente zeigten widersprüchliche Ergebnisse. Infolgedessen wurde das experimentelle Setup der LigandTracer® Experimente genauer betrachtet in Bezug auf unspezifische Bindung, potentielle Anreicherungen der Substanzen in den Zellen und ob andere Effekte vorliegen. Weitere Experimente werden nötig sein, um ein valides experimentelles Setup aufzusetzen. Weitere zukünftige Schritte umfassen die Entwicklung von weniger lipophilen Verbindungen, welche eine gleichbleibend gute Affinität und Selektivität zeigen und gleichzeitig minimale unspezifische Bindung aufweisen.

Table of content

Index of abbreviations

AChE	Acetylcholinesterase
ATI	Acetylthiocholine iodide
BCA	Bicinchoninic acid
CHO cells	Chinese hamster ovary cells
DTNB	5,5'-Dithiobis-(2-nitrobenzoic acid)
mAChR	Muscarinic acetylcholine receptor
[N-methyl-^{3}H]NMS	[N-methyl-^{3}H]Scopolaminemethylchloride
PEI	Polyethylenimine
PET	Positron emission tomography

1. Introduction

1.1. Muscarinic acetylcholine receptors

Muscarinic acetylcholine receptors (mAChRs) belong to a group of receptors known as G-protein coupled receptors. There are five different subtypes of mAChRs, which are classified into two groups.

The first group contains the subtypes M1, M3 and M5. These mAChR subtypes are found mostly in the central nervous system and are coupled with G-proteins of the Gq/G11 family. This leads for example to the release of intracellular Ca^{2+}. The receptors of this group are postsynaptic receptors and give a stimulatory impulse. (Eglen, Choppin, & Watson, 2001)

The second group contains the subtypes M2 and M4. Although these mAChR subtypes are found in the central nervous system, they also appear in the peripheral nervous system. These receptors are coupled with G-proteins of the Gi/Go-type and are found pre- as well as postsynaptically. In contrast to the first group of subtypes, the M2 and M4 receptors give an inhibitory impulse, for example to the adenylyl cyclase, which reduces the concentration of cAMP in the cytoplasm. (Eglen et al., 2001)

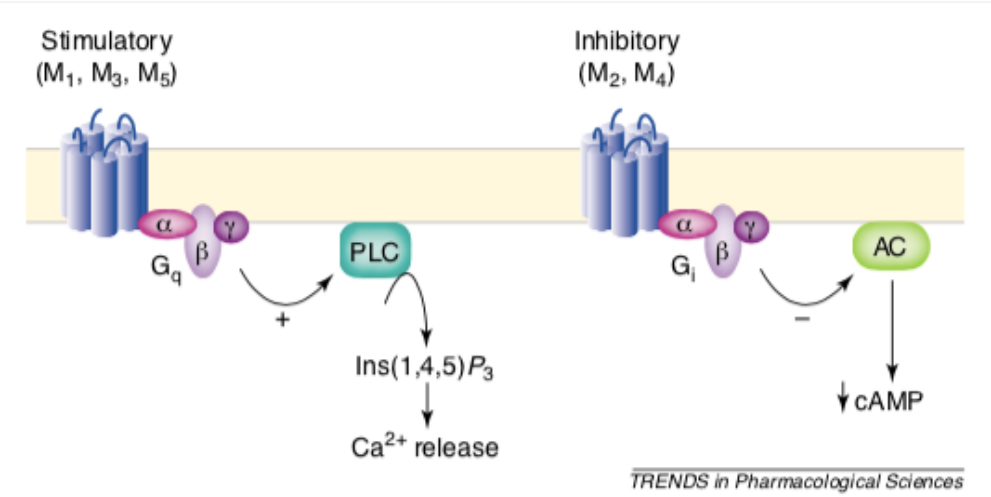

Figure 1-1: Subtypes of muscarinic acetylcholine receptors and their effects. (Eglen et al., 2001)

The M1 receptors are predominant in the central nervous system. They play an important role in learning and memorization. Therefore, agonists of the M1 receptor are possible drug candidates against Alzheimer's disease and other cognitive disorders. (Toyohara, Sakata, & Ishiwata, 2013)

The M2 receptors are the only presynaptic receptors of the mAChRs and are mostly found in the central nervous system. They regulate the release of acetylcholine and other neurotransmitters, for instance dopamine. In the neurodegenerative Alzheimer's and Parkinson's diseases, the M2 receptor slowly disappears from the cerebral cortex. This is why the M2 receptor is a potential target for the diagnosis and treatment of Alzheimer. (Toyohara et al., 2013)

In the case of the M3 receptor, its function has not been discovered yet. There is only a small amount of M3 subtype receptors and M3-knock-out mice show normal behaviour and cognitive function. (Toyohara et al., 2013)

The M4 receptor subtype is the most common subtype in the striatum. Apart from that, it also occurs in the midbrain, the cortex and the hippocampus. The M4 receptor is a postsynaptic receptor, which is usually coexpressed with dopamine D_1-receptors. Stimulation of the M4 receptor leads to a reduced dopamine release. Apart from that, the M4 receptor regulates normal cellular and synaptic activities in the striatum. Overall this makes the M4 receptor a possible target for treatment and imaging of neurological disorders, like the aforementioned Alzheimer's and Parkinson's disease or possibly even drug addiction. (Toyohara et al., 2013)

The M5 subtype is expressed in dopaminergic neurones in the substantia nigra, as well as, the ventral tegmental area. Interestingly, the M5 receptor subtype does not show a different expression in patients with Alzheimer's than in healthy people. Still, the M5 receptor could be a potential target for other neurological diseases, like Parkinson's, Schizophrenia and drug addiction. (Toyohara et al., 2013)

1.1.1. Muscarinic acetylcholine receptor protein structure

Recent crystallographic achievements allow to get a deeper insight into the structure of the mAChR binding pocket and thus allow for a rational ligand design. (Kruse et al., 2014)

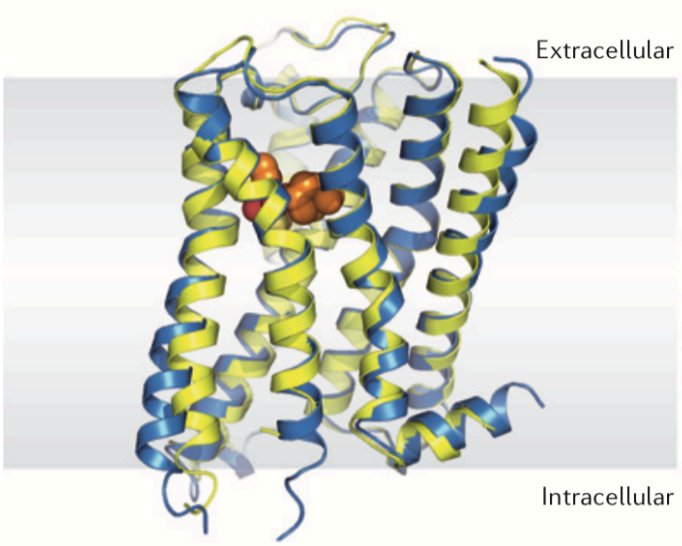

Figure 1-2 Structure of the M2 (blue) and M3 (yellow) receptor bound by an antagonist. (Kruse et al., 2014)

Figure 1-2 shows the structure of the M2 and the M3 subtype of the mAChR bound to the antagonist tiotropium. It can be seen, that the mAChR has the typical structure of a G-protein coupled receptor with seven transmembrane subunits. Additionally the figure shows how similar the different subtypes are, which increases the difficulty to develop subtype selective ligands. (Kruse et al., 2014)

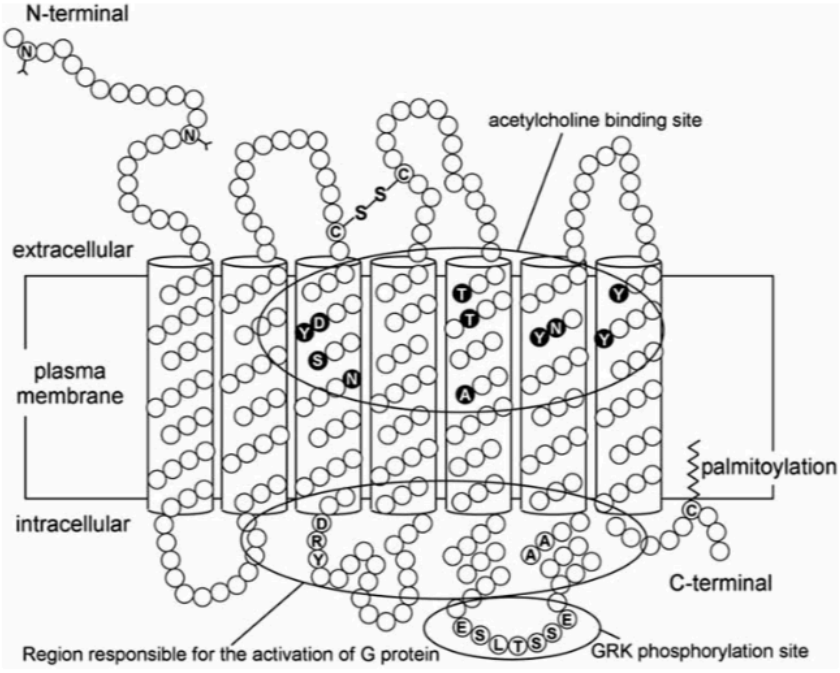

Figure 1-3: Structure of M1 mAChR. (Ishii & Kurachi, 2006)

In Figure 1-3 the schematic structure of the M1 receptor can be seen and the binding site of acetylcholine is highlighted. One of the most important features of the binding pocket is the negatively charged aspartic acid, which can be seen in the third transmembrane subunit of the receptor. (Ishii & Kurachi, 2006) The amine of the ligand binds at this position, which seems to be an important factor. As can be seen by the examples in chapter 1.1.3, all of the developed ligands contain some kind of cationic head, which binds at this position. (Kruse et al., 2014) Another important bond is the hydrogen bond between the asparagine in the sixth transmembrane subunit and the hydroxylic group of the ligand. This bond is unique to the mAChR family. (Kruse et al., 2014)

Lastly, the inclusion of large lipophilic groups, such as an aromatic ring, seem to be beneficial in developing a ligand with a high affinity for the mAChR. (Heilbronn & Bartfai, 1978)

In conclusion, the ideal candidate for a high affinity ligand targeting the muscarinic acetylcholine receptor should offer the following three structural features:

(1) a cationic head

(2) a hydroxylic group

(3) one or more aromatic rings. (Heilbronn & Bartfai, 1978)

1.1.2. Positron emission tomography

Positron emission tomography (PET) is an imaging technique used in nuclear medicine. It requires a radiopharmaceutical labelled with a positron-emitter, such as carbon-11 or fluorine-18. (Pike, 2009) The emitted positron collides with an electron outside of the nucleus, which leads to annihilation radiation. This type of radiation consists of two photons with an energy of 0.511 MeV, which are produced by the annihilation of the positron when it collides with an electron. These photons are given off at a 180° angle. The PET scanner uses the photons, which are moving in opposed directions to calculate approximately where the collision happened and in that way reconstruct an image of the tracer distribution. (Bailey, Townsend, Valk, & Maisey, 2005)

PET scans can be used in different diagnostic areas, such as cancer diagnosis, cardiology or neurology. (Bailey et al., 2005)

In the end mAChR imaging could be a way of gaining a deeper understanding of the molecular changes involved in neurodegenerative diseases like Alzheimer’s or Parkinson’s, as it was mentioned in chapter 1.1.

1.1.3. Radioactive Ligands for the mAChR

Different radiotracers for the mAChR have already been developed, though none are currently used in clinical routine for positron emission tomography (PET). In regard to the density in which the M1 and M2 receptors are estimated to be in the human brain, a suitable affinity for radiotracers for the mAChR would be around 3-50 nM. (Toyohara et al., 2013)

In overall, an ideal PET tracer targeting the human brain should have the following features:

- high affinity for the target
- selectivity for the target
- must be able to pass the blood-brain-barrier
- non-substrate for the efflux-transporter
- has no interfering radiometabolites
- very low non-specific binding
- pharmacokinetics must match the half-life of the radionuclide
- radiolabelling must be possible with the desired radionuclide, preferably with a high specific radioactivity (Pike, 2009)

The first PET imaging of mAChRs in the human brain was done in 1992, where scopolamine, which is a known mAChR antagonist, was labelled with carbon-11 and used in *in vivo* studies, first in rats and later in humans. Sadly, [^{11}C]scopolamine proofed to be not ideal, because of an unfavourable binding profile and also due the short half-life of carbon-11, which lead to a lack of an appropriate kinetic binding model for this tracer. (McPherson, 2001) These first developed tracers, like scopolamine, were all non-subtype selective and the affinity for them was too high, other examples are benztropine and dextimide. This resulted in a slow dissociation of the tracer from the receptor and in a slow permeability of the blood brain barrier. (Toyohara et al., 2013)

In 1994 tropanyl benzilate was labelled with carbon-11 and examined for PET imaging. For the first time an appropriate kinetic model could be established and reliable receptor density information could be obtained. (McPherson, 2001) Still, this PET tracer proofed difficult, because of the low blood brain barrier permeability and an affinity, which was still too high. (Koeppe et al., 1994)

The next developed radiotracers, e.g. [^{123}I](R,R)-IQNB or [^{123}I](Z)-IQNP, had a lower affinity, which made the passage through the blood brain barrier faster but also resulted in insufficient specific binding to the receptor. A lot of these tracers were labelled with iodine-123 instead of carbon-11 to allow for a longer wait after injection. (Toyohara et al., 2013)

Apart from the right affinity, it would also be ideal to have subtype selectivity. A few tracers with subtype selectivity were tested *in vitro,* for example BIBN 99, which is a selective M2

antagonist, that shows a M2/M1 selectivity of 33 to 1 *in vitro*. There are also other examples, but none of these tracers have been tested *in vivo* for their subtype selectivity. (McPherson, 2001)

There is only one reported radiotracer which shows subtype selectivity *in vivo*, [^{18}F]FP-TZTP. This radiotracer is also not used in clinics due to suboptimal kinetics. (Toyohara et al., 2013)

The structures of all of the above-mentioned radiotracers can be seen in Figure 1-4.

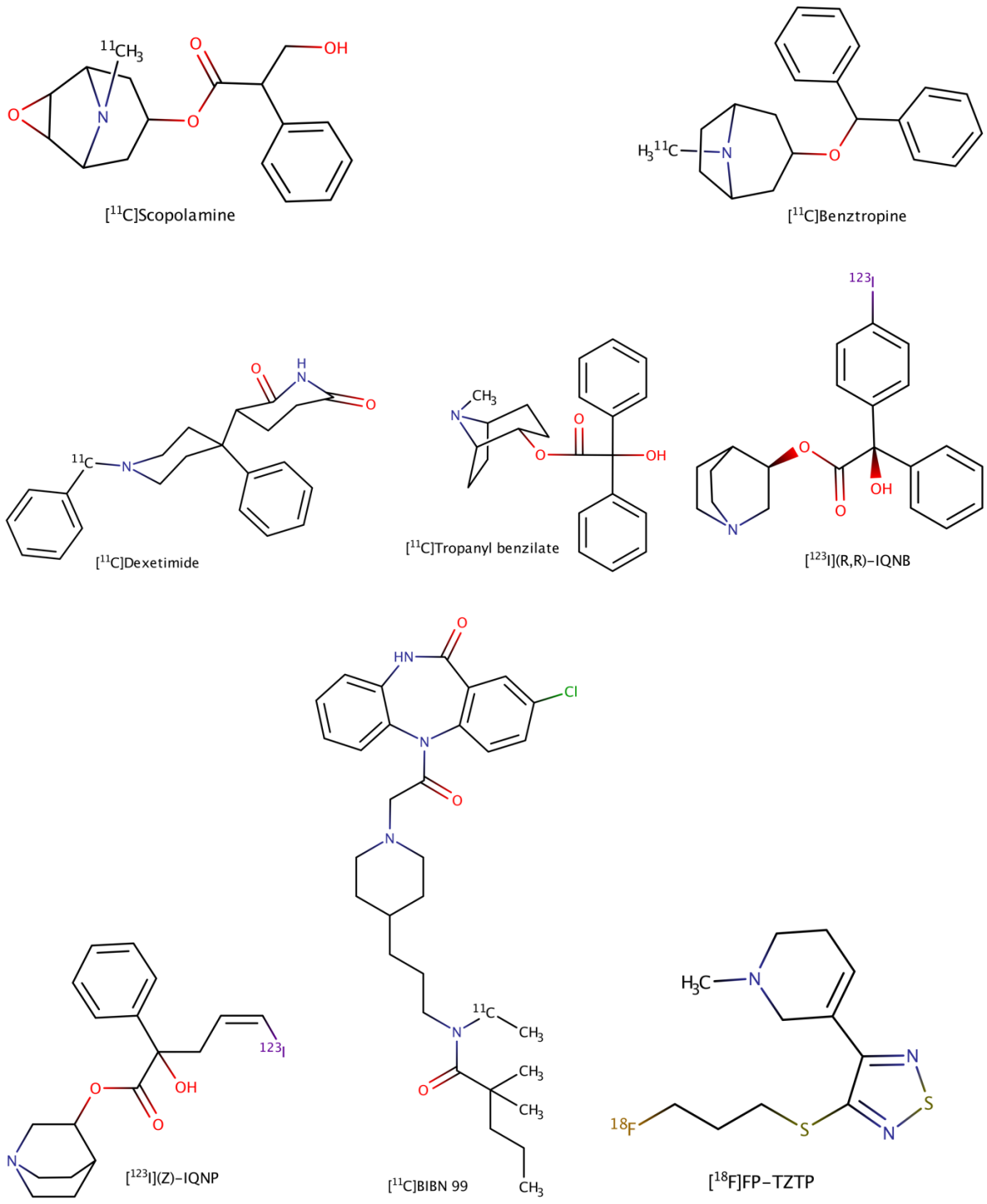

Figure 1-4: Structures of different mAChR ligands investigated as radiotracers. (McPherson, 2001; Toyohara et al., 2013)

1.2. Arecoline – a natural ligand

One of the natural occurring ligands of the muscarinic acetylcholine receptor is arecoline (Figure 1-5).

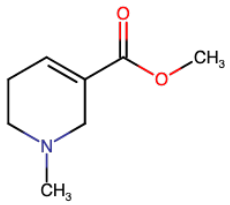

Figure 1-5: Structure of arecoline.

Arecoline is the major effective constituent of the *Areca catechu*, also known as the areca palm or betel palm. *Areca catechu* is also the fourth most commonly used drug, with its fruits, the betel nut, commonly used in traditional Chinese medicines to treat a variety of diseases including diarrhea, abdominal distension, edema and tapeworm infestation. In traditional Chinese medicines arecoline is also an indicator of the quality of the betel nut. (Liu, Peng, Hu, Xu, & Wu, 2016)

The pharmacological effects of arecoline influence a wide range of systems in the body. The most important part in all of them is the ability of arecoline to stimulate the muscarinic receptors. The effects on the central nervous system include improved cognitive function and memory in patients with Alzheimer's disease as well as alleviation of symptoms in schizophrenic patients. In the cardiovascular system arecoline shows vasodilator, antithrombotic and anti-atherogenic effects. Arecoline also shows effects in the endocrine system including the stimulation of adrenomedullary activities and stimulation of the production of testosterone. Apart from that, arecoline shows anti-parasitic effects for example against tapeworms or cysticerus.(Liu et al., 2016)

The *Areca catechu* is mainly used for digestive disorders, here arecoline is also the major effective constituent. Arecoline is promoting activity on smooth muscle contraction as well as the contraction of muscle strips of duodenum, ileum and colon. (Liu et al., 2016)

Besides all the positive effects, arecoline can also shows toxic effects dependent on the dose and consummation duration, like oral submucous fibrosis, oral squamous cell carcinoma and genotoxicity. (Liu et al., 2016)

Arecoline as a structural building block is especially promising as it offers all structural features as discussed under 1.1.3.

However, the affinity of arecoline with 15-77 µM is far too low for the application as a PET tracer. (Dong, Kameyama, Rinken, & Haga, 1995)

1.3. Radioligand binding assays

Radioligand binding assays are important experiments for developing new drugs. One of the most important area of application is the determination of the affinity of new ligands to a particular receptor. Apart from that, binding assays can also be used to determine the kinetics of the interaction. (Motulsky & Neubig, 2002)

1.3.1. Binding theory

The basis of every binding assay is a model called the law of mass action, which is based on three simple ideas. The first is, that the ligand and the receptor collide due to diffusion and then the binding occurs. This association is described by the association constant k_{on}. In the next step, the ligand and the receptor dissociate after a certain amount of time has passed. The dissociation is described by the dissociation constant k_{off}. In the end, both the ligand and the receptor remain the same as before the binding. This model can be described by Equation 1-1. (Motulsky & Neubig, 2002)

$$ligand + receptor \rightleftharpoons ligand \cdot receptor$$

Equation 1-1: Theory of mass action.

To determine the affinity of a ligand, the equilibrium has to be reached. In this case, the rate of new ligand-receptor complexes formed equals the rate of dissociation of these complexes. This gives Equation 1-2, which can be rearranged to form the equilibrium dissociation constant K_d (Equation 1-3). (Motulsky & Neubig, 2002)

$$[ligand] \times [receptor] \times k_{on} = [ligand \cdot receptor] \times k_{off}$$

Equation 1-2

$$\frac{[ligand] \times [receptor]}{[ligand \cdot receptor]} = \frac{k_{off}}{k_{on}} = K_d$$

Equation 1-3

The K_d is a measure of the affinity of a ligand to the receptor. When the K_d is low, the concentration of ligand-receptor-complex is high and the concentrations of free ligand and free receptor are low, which means less ligand is needed to occupy the receptors and the affinity is

high. For a high K_d the opposite is true, which means the affinity is low. (Motulsky & Neubig, 2002)

Since the law of mass action is only a model, there are a few limitations to be considered. On one hand, there are four assumptions, which the model makes, that may not be true for the real experiment. These assumptions are, that

(1) the receptors are all equally accessible for the ligands,

(2) no partial binding occurs,

(3) all binding is reversible,

(4) the ligand and the receptor are not altered by the binding. (Motulsky & Neubig, 2002)

Apart from that, it is also important to consider, that there are no standard conditions for binding assays and that they may be done under non-physiological conditions. Even if that is not the case, it is still important to consider, that factors such as metabolism or non-specific binding could occur under *in vivo* circumstances. (Davenport & Russell, 2011)

1.3.2. Competitive binding assays

In competitive binding experiments, a fixed concentration of a radioligand with high affinity is employed, while different concentrations of an unlabeled ligand with unknown affinity are applied until the radioligand is completely displaced. A sketch of a typical sigmoidal course of the results of such an experiment can be seen in Figure 1-6. (Motulsky & Neubig, 2002)

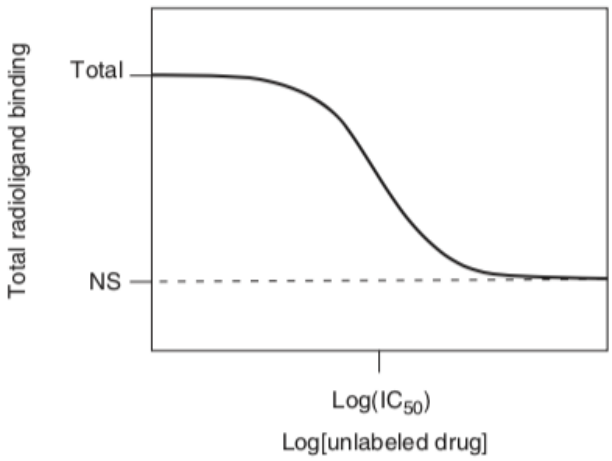

Figure 1-6: Schematic of a competitive binding experiment. (Motulsky & Neubig, 2002)

The upper part of the graph shows the amount of radioligand bound, when no other ligand is present, whereas the bottom shows the amount of non-specific binding. The inhibitory concentration 50%, IC_{50}, is the inflexion point of the graph. This is the point where the

unlabeled ligand blocks half of the specific binding of the radioligand. The IC_{50} is dependent on three factors, the affinity of the radioligand to the receptor (K_d), the concentration of the radioligand used and the K_i. The K_i is the concentration at which the unlabeled ligand would be bound to half of the binding sites in absence of a competitor. (Motulsky & Neubig, 2002) Since the IC_{50} is dependent on the concentration of radioligand used, it is not practical to use it for comparing between different experimental setups. For this case the K_i is used, which can be calculated using the Cheng-Prussoff-equation (Equation 1-4). (Motulsky & Neubig, 2002)

$$K_i = \frac{IC_{50}}{1 + \frac{[radioligand]}{K_d}}$$

Equation 1-4: Cheng-Prussoff-equation.

In the Cheng-Prussoff-equation IC_{50} is the one obtained in the experiment for the unlabeled ligand, whereas K_d is the known K_d value of the radioligand.

1.3.2.1. Filtration method

In order to study the affinity of a ligand towards a receptor, cellular membranes containing the molecular target in high concentration have to be prepared. Target membranes can be obtained by lysis of suitable cells and subsequent centrifugation. The way the cell lysate is centrifuged, is dependent on the location and the abundance of the receptor. (Keen & Qume, 2003)

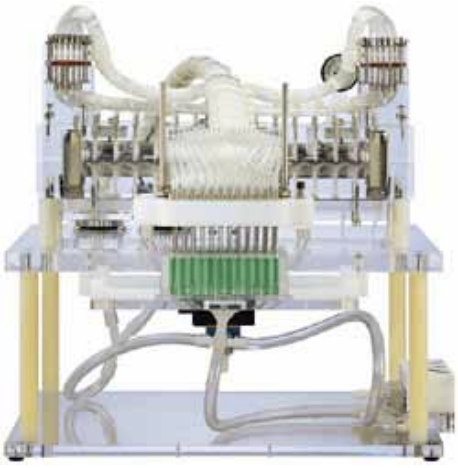

Figure 1-7: Brandel Cell Harvester. (http://www.brandel.com/graphics/harvestersilh250.jpg; accessed on 17.05.2019.

In case of a competitive binding assay the radioligand, the competing ligand and the membrane suspension are incubated in a buffer. The next step is the separation of the bound ligand from the free ligand, which can be accomplished in different ways, like centrifugation, gel filtration, precipitation or adsorption. In the case of the filtration method the separation is accomplished

by filtration. The filtration can be done by hand or with the help of a commercially available filtration system, for example a Brandel Cell Harvester. (Figure 1-7) The bound ligand remains on the filter by adhesion and the filter can be incubated in a liquid scintillant and later measured by liquid scintillation counting. The main disadvantage of filtration is the possibility of nonspecific binding to the filter. This can be rectified by pretreating the filter with antiadsorbants, such as polyethylenimine (PEI). (Keen & Qume, 2003)

1.3.3. Ellman assay

The Ellman assay is named after the Ellman reagent, which is 5,5'-dithiobis-(2-nitrobenzoic acid) or simply DTNB. (Ellman, 1959) DTNB is used for its reaction with thiol-groups, which leads to a yellow anion. In the spectrophotometric Ellman assay, this reaction is used to measure the amount of acetylthiocholine cleaved by the acetylcholinesterase. (Worek, Eyer, & Thiermann, 2012)

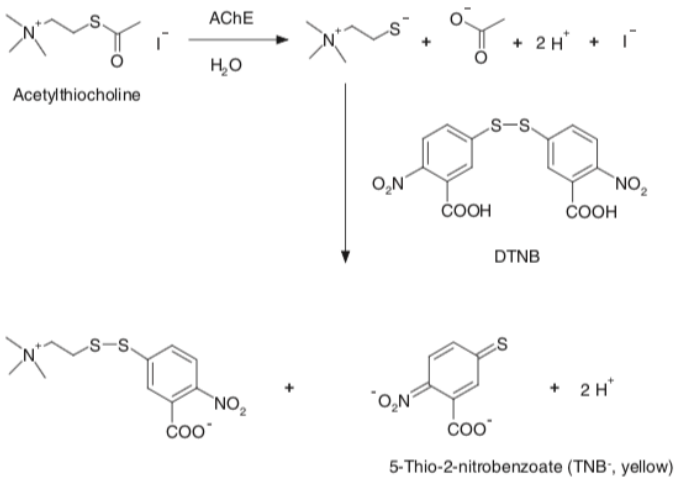

Figure 1-8: Reaction scheme of the Ellman assay. (Worek et al., 2012)

In this thesis the Ellman assay was used to determine if the arecoline derivatives inhibit the off-target acetylcholinesterase. In this case if the arecoline derivatives would inhibit the acetylcholinesterase, the ATI would not get cleaved and therefore the cleaved product could not react with DTNB to form the yellow anion. This means, that with increased concentration of arecoline derivative the colour intensity of the solution would change. This change in colour intensity can then be measured with a photometer.

1.3.4. LigandTracer®

The LigandTracer® is an instrument developed by Ridgeview, which allows to monitor the binding of a radioligand to receptors on cells in real time. It is therefore a useful tool to determine the kinetic interactions of a radioligand with the receptor. (Ridgeview, 2019)

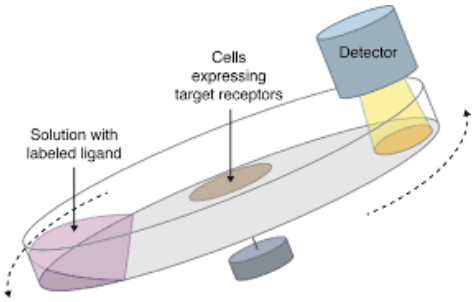

Figure 1-9: Layout of a LigandTracer®. (Ridgeview, 2019)

For an experiment cells need to be seeded in one half of a petri dish and need to be confluent. The petri dish is later put onto the LigandTracer® and is continuously rotated. The baseline is measured with fresh medium and after that a solution of the radiolabeled ligand is added. Since the detector measures the upper part of the tilted plate (Figure 1-9), the medium containing the free ligand is never measured. Instead, the cells are measured, which bind the ligand and the binding kinetics can be seen in real time. (Ridgeview, 2019)

The resulting curve is later fitted with a model, that gives the observed rate constant k_{obs}, which shows how quickly an equilibrium is reached. Since the observed rate constant of a bimolecular reaction is defined by Equation 1-5, it is possible to get the k_{off} and k_{on} as the intercept and the slope of a linear relationship between k_{obs} and the radioligand concentration using different experiments with the same ligand in different concentrations. (Motulsky & Neubig, 2002)

$$k_{obs} = k_{off} + k_{on} \times [radioligand]$$

Equation 1-5: Relationship between k_{obs} and k_{on}, as well as, k_{off}. (Motulsky & Neubig, 2002)

2. Aim

As the muscarinic acetylcholine receptors are an interesting target for diagnostic studies using PET technology, it is therefore interesting to develop respective radiotracers. Ideally those tracers should not only bind with an affinity of around 3-50 nM to the mAChRs but should also show high subtype selectivity. (Toyohara et al., 2013)

To find new ligands, which could potentially be used for brain imaging of the muscarinic acetylcholine receptor structures based on the arecoline scaffold were developed offering the ideal features for radiotracers with sufficient blood-brain-barrier penetration, as described under 1.1.3. (Figure 2-1, unpublished data)

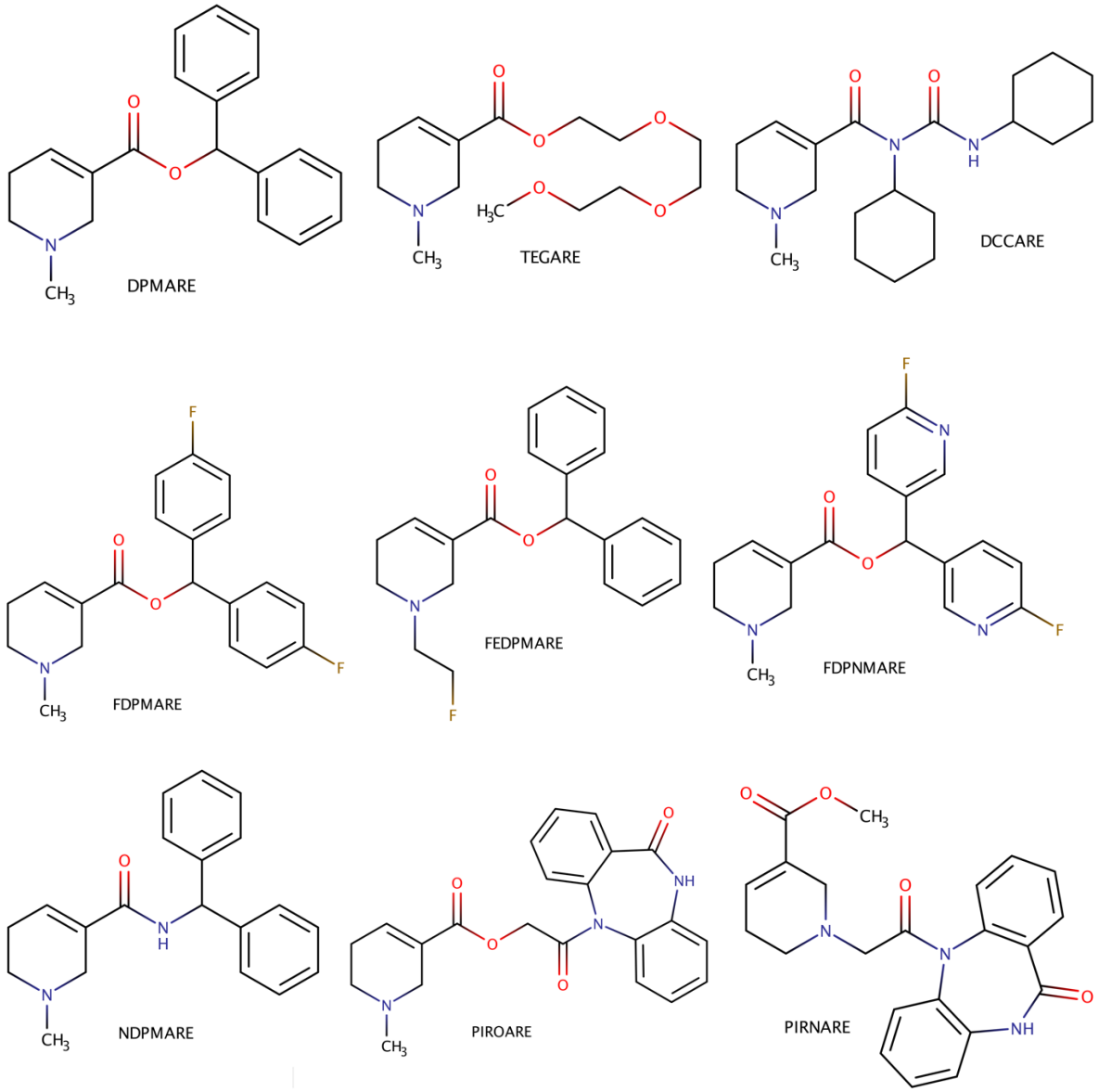

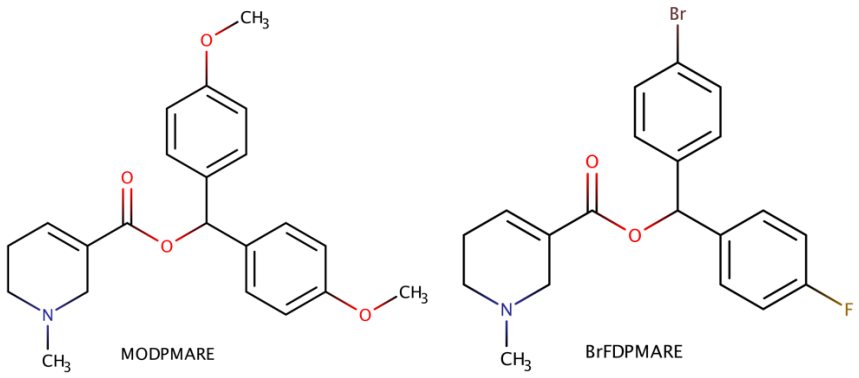

Figure 2-1: Structures of arecoline derivatives.

In light of that, the purpose of this thesis was to evaluate pharmacological parameters of these set of arecoline-based compounds. Therefore, the binding properties are in the main focus. From the results, a trend should be drawn in order to find suitable structures for further testing. Consequently, at first the K_i values of the arecoline derivatives should be determined using the filtration method. Furthermore, to prove that the arecoline derivatives do not bind to the off-target acetylcholinesterase, the interaction of the arecoline derivatives to the acetylcholinesterase should be tested. At first, the inhibition of the acetylcholinesterase will be tested using an Ellman assay. In the next step, the ability of the acetylcholinesterase to cleave the arecoline derivatives will be further analysed by using an HPLC method. In the end, the most promising arecoline derivatives will be chosen for investigating their kinetic interaction with the mAChR using LigandTracer®.

3. Experimental part

3.1. Materials

3.1.1. Reagents

- Arecoline derivatives synthesized by Marius Ozenil, M.Sc.
    - DPMARE
    - TEGARE
    - DCCARE
    - FDPMARE
    - FEDPMARE
    - FDPNMARE
    - NDPMARE
    - PIROARE
    - PIRNARE
    - MODPMARE
    - BrFDPMARE (enantiomers separated by HPLC using AGP 0.3 cm x 5 cm 5 µm)
- Acetonitrile (CAS: 75-05-8, Sigma Aldrich)
- Acetylcholinesterase (CAS: 9000-81-1, Sigma Aldrich)
- Acetylthiocholine iodide, ATI (CAS: 1866-15-5, Sigma Aldrich)
- Pierce™ BCA Protein Assay Kit (Thermo Fisher Scientific)
- CHO-K1 cells, stably transfected with human muscarinic receptors M1-M5 (Missouri University of Science and Technology cDNA Resource Center (Cell Catalog#: CEM1000000, CEM2000000, CEM3000000, CEM4000000, CEM5000000))
- Dimethyl sulfoxide, DMSO (CAS: 67-68-5, Sigma Aldrich)
- 5,5'-Dithio-bis-(2-nitrobenzoicacid), DTNB (CAS: 69-78-3, Carl Roth)
- Ethylenediaminetetraacetic acid, EDTA (CAS: 60-00-4, Sigma Aldrich)
- Geneticin (Life Technologies Limited)
- Gibco Fetal Bovine Serum, FBS (Life Technologies Limited)
- Gibco Dulbecco's Phosphate-Buffered Saline, PBS (Life Technologies Limited)
- L-Glutamine (Life Technologies Limited)
- Medium Gibco F-12 (1x) Nutrient Mixture (Ham) (Life Technologies Limited)
- Methanol (CAS: 67-56-1, Merck Millipore)
- $MgCl_2$ (CAS: 7791-18-6, Merck Millipore)

- Na_2HPO_4 (CAS: 10028-24-7, Sigma Aldrich)
- NaH_2PO_4 (CAS: 10049-21-5, Merck Millipore)
- $(NH_4)H_2PO_3$ (CAS: 7722-76-1, Sigma Aldrich)
- [*N*-methyl-^{3}H]Scopolaminemethylchloride, [*N*-methyl-^{3}H]NMS (Perkin Elmer, 37 MBq, 2.964 TBq/mmol in 1 mL ethanol)
- Poly(ethyleneimine) solution, PEI (CAS: 9002-98-6, Fluka Analytical)
- Protease inhibitor P2714 (Sigma Aldrich) dissolved in 10 mL Milli-Q water and stored at -20 °C
- Tacrine (CAS: 1684-40-8, Santa Cruz)
- Tris(hydroxymethyl)aminomethane (CAS: 77-86-1, Merck Millipore)
- Trypsin 0.05% (Life Technologies Limited)
- Ultima Gold™ (Perkin Elmer)

3.1.2. Equipment

- BioTek Synergy HTX multi-mode reader
- Brandel cell harvester
- Hidex 300 SL
- HPLC:
    - Column: XSelect® HSST 33.5 µm, 4.6x100 mm
    - Detector and autosampler: Agilent Technologies 1100 series
    - Deaerator and pump: Agilent Technologies 1200 series
- LigandTracer® grey and yellow
- Olympus XC50
- Sorvall Ultracentrifuge Combi (DuPont)
    - Sorvall No.11510 rotor

3.1.3. Software

- Microsoft Excel 2013
- GraphPad Prism 6
- LigandTracer Control
- MikroWin 2000

3.2. Methods

3.2.1. Cell culture

3.2.1.1. Splitting

The Chinese hamster ovary (CHO) cells, which were stably transfected with the different subtypes of mAChR, were cultivated in cell culture flasks and since CHO cells are adherent, once they reach 80-90% confluency, they have to be split in order to resume exponential growth. Therefore, the old medium was taken off and the cells were washed once with DPBS. Then, trypsine was added to detach the cells from the bottom of the flask. Therefore, the flask was put into the incubator for approximately 5 minutes. Afterwards medium was added to deactivate the trypsine and the cells were seperated from each other by repeated pipetting. Depending on how high the cells should be split, a part of the suspension was taken out of the flask and the flask was refilled with fresh medium. In the end, the cells were suspended with the flask to assure a proper distribution of the remaining cells. The cell culture flasks were put back into the incubator at 37°C, humidified with 5% CO_2.

3.2.1.2. Preparation of membranes

For the preparation of membranes, which would later be used in the binding experiments, cells transfected with the desired mAChR subtype were cultivated in ten T175 flasks. The cells were grown to at least 80% confluency to assure a sufficient amount of target.

First, the flasks were put on ice and the old medium was removed, after which the cells were washed once with DPBS, in order to remove dead cells and traces of medium. Then 2 mL of ice cold buffer, containing 10 mM Tris/HCl and 1 mM EDTA at pH 7.4, was added and the cells were scraped off using a cell scraper. The resulting suspension of two T175 flasks was transferred into 5 mL Eppendorf tubes, which already contained 400 µL protease inhibitor. The content of the Eppendorf tube was homogenized by pushing it through an insulin needle. The Eppendorf tubes were centrifugated at 1000 g for 10 minutes at 4 °C. Then the supernatant was transferred into SETON-tubes and centrifugated in the ultracentrifuge at 106160 g for 40 minutes at 4 °C. Again, the supernatant was removed, and the pellet was dissolved in a 50 mM Tris/HCl buffer pH 7.4. The membrane solution was then filled into cryovials and stored at -80 °C.

3.2.1.3. Determination of protein concentration

To determine how much of the membrane suspension, produced as described in 2.2.1.2., should be used for the following binding experiments, it is necessary to know how much protein the suspension contain. For that purpose, the protein concentration was determined using a BCA kit.

In the beginning the albumin standards and the working reagent were mixed, as described in the user guide of the BCA kit. To determine the protein concentration the microplate procedure was used, as the sample size was limited. Therefore, 25 µL of each standard and each unknown sample of membrane suspension was pipetted into a 96-well plate and 200 µL of working reagent were added to each well. In parallel, the standards were used to create a standard curve on the same 96-well plate, which allowed to determine the protein concentrations of the membrane solutions. The plate was incubated for 30 minutes at 37°C and then left to cool to room temperature, before measuring the absorbance in a photometric plate reader at 562 nm.

3.2.2. Binding assays

3.2.2.1. Harvester

At first the arecoline derivative, which should be tested, was dissolved in DMSO and a dilution series, which usually covered a range in between a concentration of 1 mM and 100 nM, was made. Then 5 µL from five different concentrations, as well as pure DMSO (blank) and a 100 µM solution of scopolamine in DMSO (positive control) were pipetted into test tubes. The radioligand [*N*-methyl-^{3}H]scopolaminemethylchloride ([*N*-methyl-^{3}H]NMS), which was used in this replacement experiment, was dissolved in a buffer solution of 50 mM Tris, 10 mM $MgCl_2$ and 1 mM EDTA in distilled water with a pH of 7.4. The radioligand was dissolved in different concentrations according to the subtype of receptor used in the experiment (Table 3-1).50 µL of the radioligand solution was pipetted into the test tubes. The membrane suspension, containing the subtype of mAChR were dissolved in the same buffer, as was used for dissolving the radioligand. Then 445 µL of the diluted membrane suspension was pipetted into the test tubes, which were then thoroughly mixed and left to incubate for 1.5 hours at 20 °C.

	M1	M2	M3	M4	M5
Concentration of radioligand	2 nM	3 nM	8 nM	2 nM	10 nM
Amount of membrane solution used	90 – 150 µL	150 – 400 µL	90 – 200 µL	150 – 300 µL	150 – 200 µL

Table 3-1: Amount of radioligand and membrane suspension used in the radioligand binding assay.

In the meantime, the GF/B filter was blocked with a 0.5% solution of PEI in distilled water. Before the filtration, the cell harvester was washed using ice-cold washing buffer, which was a solution of 50 mM Tris in distilled water at pH 7.4. After the incubation period the mixtures were filtered using a cell harvester and the test tubes were washed two times using the ice-cold washing buffer. Afterwards, the filter was punched out and was put into the beta counter test tubes. Then 2 mL of the scintillation cocktail was added. The test tubes were shaken for 10 minutes and measured in the beta counter with a counting time of 60 s and the activity type set to low, H-3, beta. The beta counter measured counts per minute (cpm).
The resulting data (cpm) were analysed with GraphPad Prism 6, where they were plotted against the logarithms of the concentrations. The curve was fitted using "One Site – Fit IC50", which gave the IC_{50} value. To calculate the IC_{50}, the program uses the following equation (Equation 3-1), where "bottom" and "top" stand for the plateau on the y-axis.

$$y = bottom + \frac{top - bottom}{1 + 10^{x - \log(IC_{50})}}$$

Equation 3-1

Later the Cheng-Prusoff equation was used to calculate the K_i value.

3.2.2.2. Acetylcholinesterase inhibition assay

To determine if the samples were inhibitors of acetylcholineesterase, an Ellman Assay was performed according to protocol by Darras *et.al.* (Darras & Pang, 2017)
The enzyme for the inhibition assay was at first diluted using a mixture of 20 mM NaH_2PO_4 and 20 mM Na_2HPO_4 in a 4:6 ratio at pH 8.0, which lead to a 1 mg/mL solution. For the assay it was necessary to find out which enzyme concentration to use. Therefore, the enzyme solution was again diluted in the same buffer to get the serial concentration series for further testing. 250 µL of the different enzyme solutions were then diluted using 13.5 mL of a 50 mM NaH_2PO_4 buffer at pH 8.0, which gave the final concentrations. For the Ellman Assay it was

desirable that the kinetic of the reaction, which was observed by absorbance measurements, does not show a plateau over a period of at least 10 minutes. With this in mind, the different enzyme solutions were tested in combination with the highest concentration of ATI (3 mM) and with a 0.5 mM solution of DTNB. In the end the final enzyme concentration of 0.0682 µg/mL proved to be ideal for this experimental setup.

The different arecoline derivatives had already been dissolved in DMSO in a concentration of 10 mM. As was shown by Kumar *et.al.*, DMSO is an inhibitor to human acetylcholinesterase, consequently the solutions were prediluted to 1 mM using distilled water. (Kumar & Darreh-Shori, 2017) From these solutions 5 µL were pipetted in two columns of a 96-well-plate. In the first two columns distilled water was used as a blank. Then 200 µL of the enzyme solution (0.0682 µg/mL) were added column after column. After 4 minutes 48.8 µL of DTNB (0.5 mM) were added. The next step was the addition of 48.8 µL of a different concentration of ATI (3 mM, 1.5 mM, 0.75 mM, 0.375 mM or 0.1876 mM) for each row after another minute. Two minutes later the plate was placed in the photometric microplate reader, where the absorbance was measured in 10 second intervals for 10 minutes at 405 nm.

The assay was validated by using tacrine as a reference standard of known binding affinity. The results were than compared to the range of values found in the literature.

3.2.2.3. Acetylcholinesterase cleavage experiments

Additionally, to verify that the arecoline derivatives were no substrate to the acetylcholinesterase, a HPLC method was applied. For the HPLC, 100 µL of a solution containing the similar concentration of the arecoline derivative and the enzyme as used in the Ellman Assay, was prepared. The same solution was prepared for the blank using distilled water instead of the enzyme solution. Then the reaction was quenched with 100 µL of acetonitrile/methanol 1:1 after 10 minutes. Apart from that the experiment was repeated with a longer timeframe of 60 minutes. After quenching, the substances were analysed by HPLC using a gradient method.

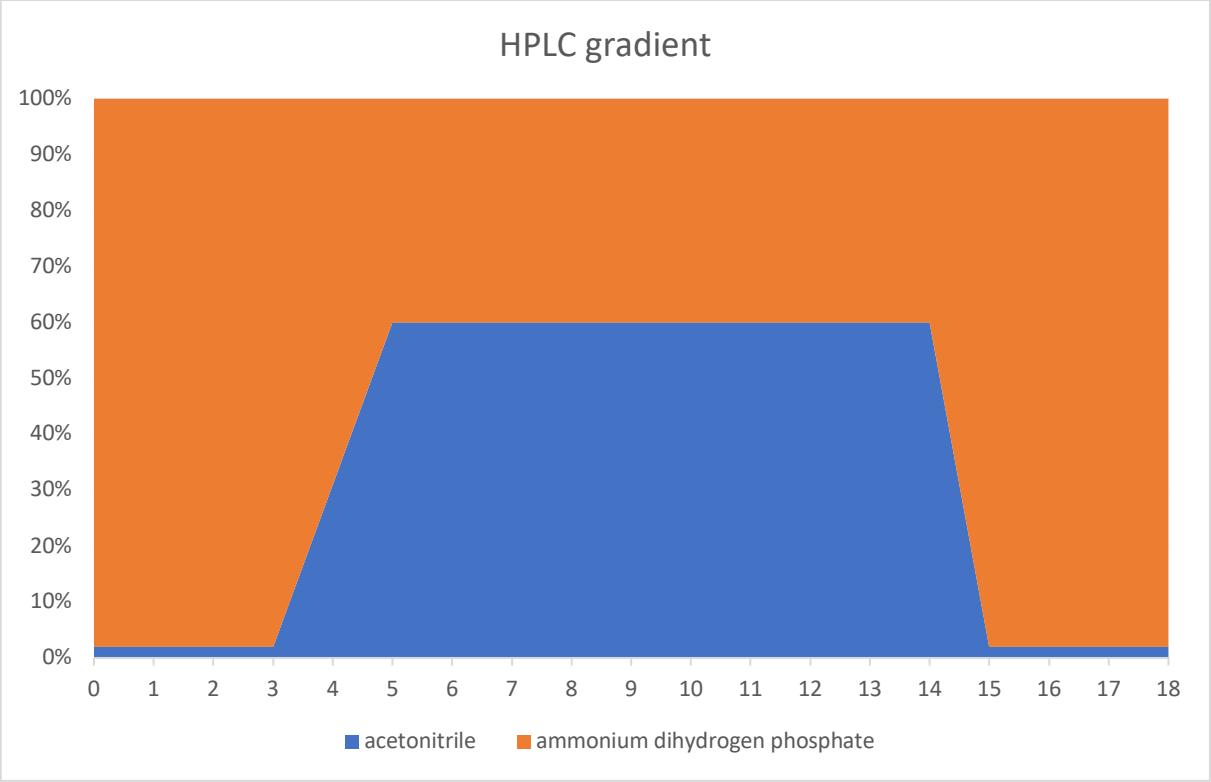

Figure 3-1: HPLC gradient used in the acetylcholinesterase cleavage experiments.

The gradient consisted of 2% acetonitrile and 98% $(NH_4)H_2PO_3$ (25 mM, pH=9.3) for the first three minutes. From minute 5 to minute 14 60% acetonitrile and 40% $(NH_4)H_2PO_3$ (25 mM, pH=9.3) were used. In the end the mixture was again changed to 2% acetonitrile and 98% $(NH_4)H_2PO_3$ (25 mM, pH=9.3) from minute 15 onwards. A linear gradient was set up for the eluent composition between 3-5 min and 14-15 min, see Figure 3-1. Finally, to prove that the acetylcholinesterase did not cleave the tested arecoline derivative, the corresponding peaks were compared to the blank and a reference standard of arecaidine.

3.2.2.4. Ligand Tracer®

In the next step the kinetics of the binding of arecoline derivatives to the muscarinic acetylcholine receptor in living cells was tested using LigandTracer®.

In order to seed the CHO cells, transfected with the desired mAChR subtype, in one half of a petri dish, one million cells were suspended in a volume of 1 mL and pipetted on an area of 1 cm^2 close to the edge of the petri dish. Overnight the cells attached to the bottom of the petri dish and got 100% confluent, which is necessary when using the LigandTracer®. For the background measurement, the petri dish was put on the LigandTracer®. Before the measurement was started, the medium was taken off and replaced by 3 mL fresh medium. The petri dish was then left to rotate for at least 30 minutes to get a stable background measurement.

Then a defined volume of ^{11}C-labeled arecoline derivatives formulated in 6 mL PET-PP + NaCl, 10 mL 0.9% NaCl and 1.5 mL ethanol was added to the medium in the petri dish. Different concentrations of the arecoline derivatives were tested, starting with the lowest, which was 10 times smaller than the K_i found by the harvester experiments, and ranging up to 10 times higher than the K_i. After the addition of the arecoline derivative it was necessary to wait until the system reached equilibrium. This took between 8 to 15 minutes, depending on the concentration and the arecoline derivative used. In some cases, at this point cold scopolamine (10 μM in H_2O) was added to see if the arecoline derivative would be displaced. In other cases, the medium was replaced by fresh medium to monitor the dissociation as well.

All data was analysed by GraphPad Prism 6 and the data points are shown with the standard deviation. The statistical analysis was performed in GraphPad Prism 6 using a Dunett's multiple comparison test with a 2way ANOVA.

4. Results and discussion

4.1.1. Determination of protein concentration

At first the measured absorbance of the standard dilution series of albumin was plotted against the concentration. This standard curve can be seen in Figure 4-1.

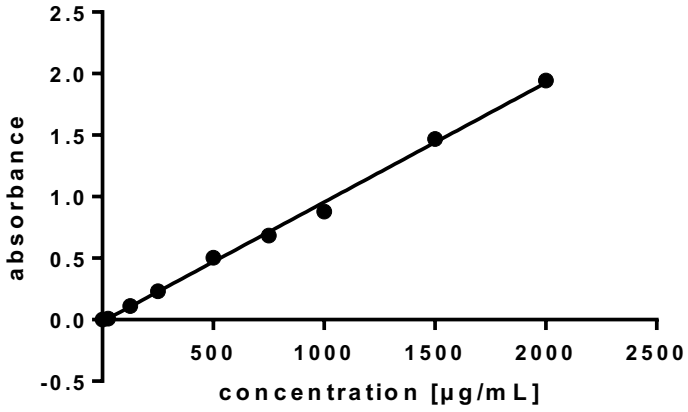

Figure 4-1: Standard curve of albumin.

In the next step the concentration of the observed absorbance for the samples was derived from the standard curve. As it is shown in Table 4-1 the protein concentrations were all in the range of 500 µg/mL.

	M1	M2	M3	M4	M5
Protein concentration [µg/mL]	512 ± 19	598 ± 22	460 ± 80	607 ± 11	494 ± 98
cpm plateau approximately for 100 µL membrane solution used	550 - 600	100	500 - 600	500 - 550	400 - 450
Expression of receptor in cells [pmol/mg]	5.5	2.9	2.2	3.1	2

Table 4-1: Comparison of protein concentrations according to the BCA kit, the approximate cpm measured during the harvester experiments for 100 µL of membrane solution used and the expression of the receptor in the cells according to the information provided in the cell catalog (Missouri University of Science & Technology, 2010a, 2010b, 2010c, 2010d, 2010e).

Interestingly the protein concentrations of the different membrane solutions didn't show a direct relation to the later discovered plateaus in the harvester experiments, see Table 4-1. In M3 the

protein concentration was lowest, but the plateau in the harvester experiment was usually found at around 500-600 cpm per 100 µL of membrane solution used. Whereas the protein concentration of M2 was second highest but only showed around 100 cpm per 100 µL of membrane solution. The other three subtypes showed very similar plateaus as the M3 did. M1 had 550-600 cpm per 100 µL of membrane solution, M4 had 500-550 cpm per 100 µL of membrane solution and M5 had 400-450 cpm per 100 µL of membrane solution, respectively. This shows that there is no direct correlation between the protein concentration determined with the BCA kit and the height of the plateau measured in the harvester experiments. The reason for this difference maybe because lipids interfere with the BCA assay, according to the instructions of the kit (Thermo Fisher Scientific, 2011).

Apart from that, the different plateau heights were also compared to the amount of receptor expressed on the cells as stated in the corresponding cell catalogue (Missouri University of Science & Technology, 2010a, 2010b, 2010c, 2010d, 2010e). Again, no direct correlation could be found (Table 4-1), although the M1 membrane solution has the highest plateau and the corresponding cells have the highest expression of receptor. For the M2 receptor, which has by far the lowest plateau, the expression of the receptor is still average. The discrepancies could be due to the flasks not being equally confluent at the time the membrane solutions had been prepared.

4.1.2. Harvester experiments

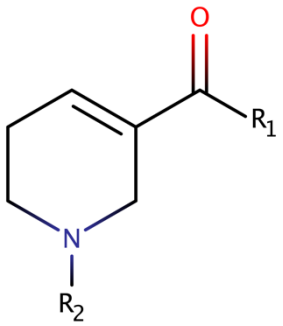

Figure 4-2: Scaffold of the tested structures. For the different residues see Table 4-2.

	R_1	R_2
DPMARE	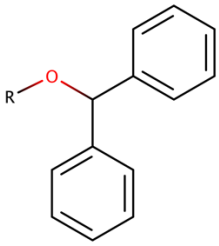	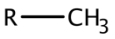
TEGARE	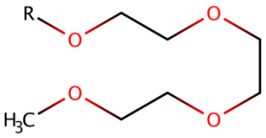	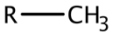
DCCARE	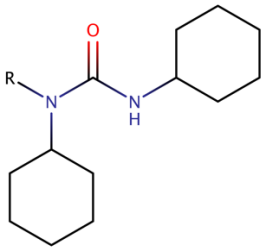	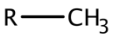
FDPMARE	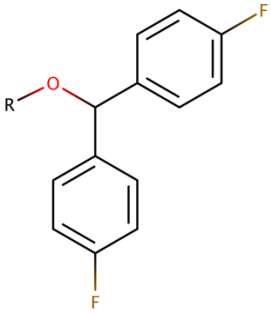	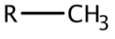
FEDPMARE	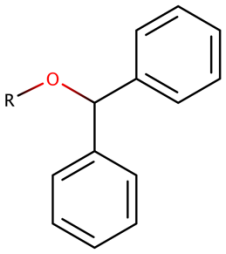	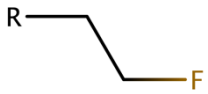
FDPNMARE	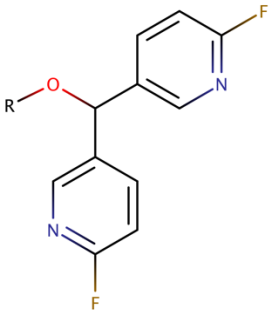	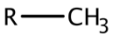

NDPMARE	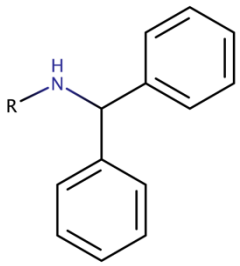	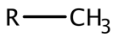
PIROARE	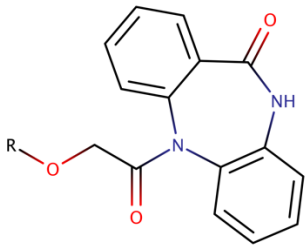	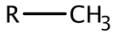
PIRNARE	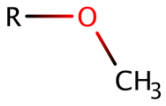	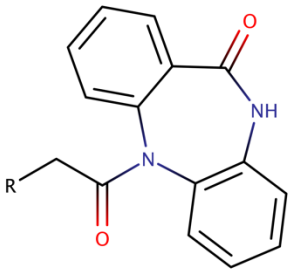
MODPMARE	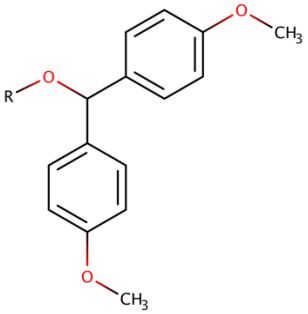	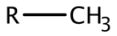
BrFDPMARE	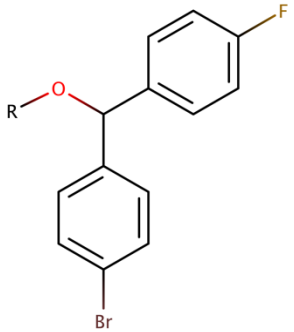	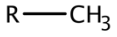

Table 4-2:Residues of the structure shown in Figure 4-2.

The data acquired by the beta-counter was plotted against the logarithms of the competitor concentrations in GraphPad Prism 6. Examples of typical experiments for the different subtypes

of mAChRs can be seen in Figure 4-3, Figure 4-4 and Figure 4-5, in all of these cases FDPMARE was the tested ligand.

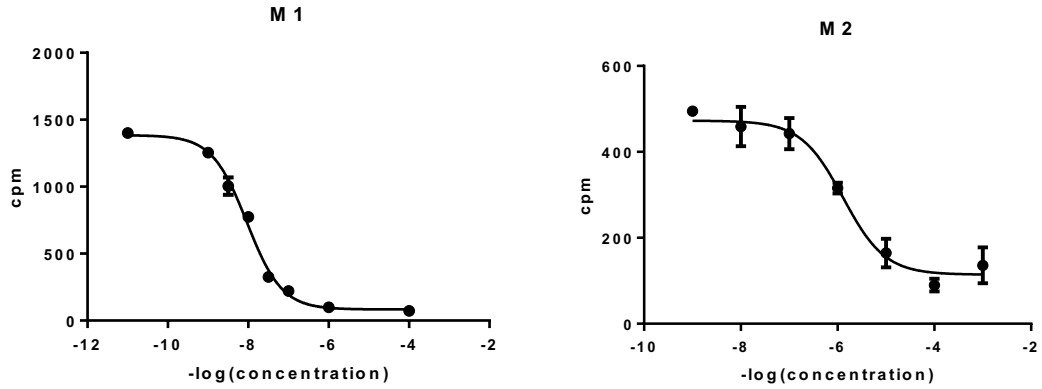

Figure 4-3: Example for an experiment with mAChR M1 and M2 using FDPMARE.

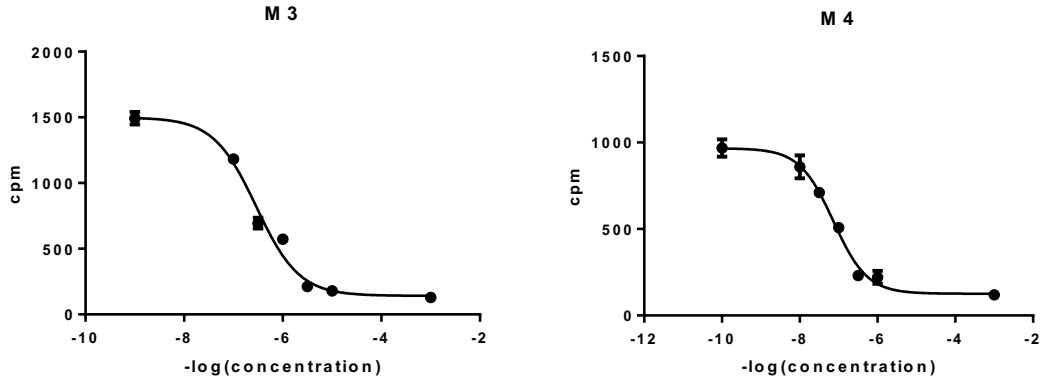

Figure 4-4: Example for an experiment with mAChR M3 and M4 using FDPMARE.

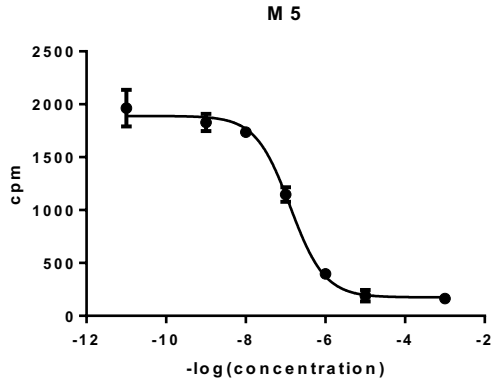

Figure 4-5: Example for an experiment with mAChR M5 using FDPMARE.

The curves seen in these examples were fitted using the "One Site – Fit IC50", which uses the following equation (Equation 4-1) to calculate the IC_{50} values.

$$y = bottom + \frac{top - bottom}{1 + 10^{x - log\,(IC_{50})}}$$

Equation 4-1

Later the IC_{50} values were used to calculate the corresponding K_i values. For this purpose, the Cheng-Prusoff-equation (Equation 4-2) was used. (Cheng & Prusoff, 1973)

$$K_i = \frac{IC_{50}}{\frac{[A]}{K_D} + 1}$$

Equation 4-2: Cheng-Prusoff equation for inhibition constants at cellular receptors.

Here [A] stands for the concentration of radioligand used and K_D stands for the K_D value of the radioligand used. For [*N*-methyl-^{3}H]NMS the K_D values are stated in Table 4-3. (PerkinElmer, 2009a, 2009b, 2009c, 2009d, 2009e)

	M1	M2	M3	M4	M5
K_D [nM]	0.17	0.15	0.16	0.07	0.16

Table 4-3: K_D values for [N-methyl-^{3}H]NMS for the different mAChR subtypes.

The resulting K_i values for the different samples, as well as the K_i values for arecoline, are shown in Table 4-4.

Figure 4-6 shows experiments with the M1 subtype of mAChR with the different samples tested. It shows clearly the different binding affinities towards the receptor.

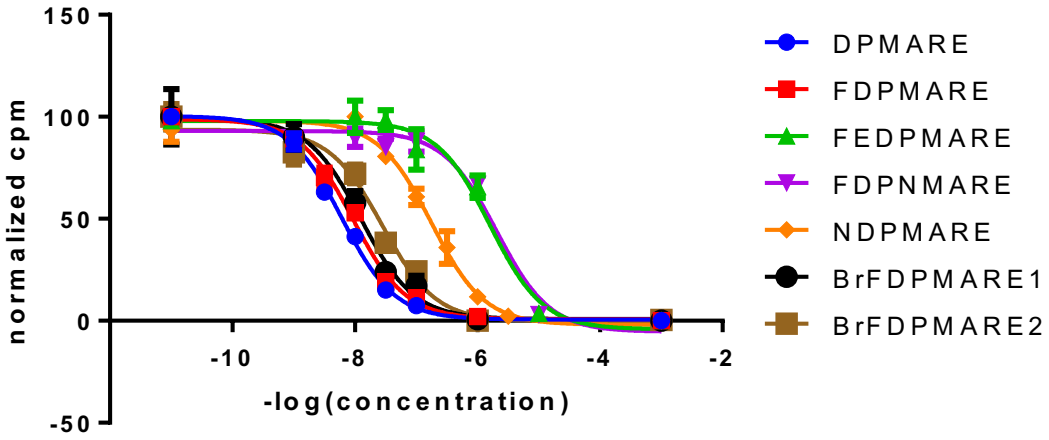

Figure 4-6: Comparison of the binding affinities of the different structures to the mAChR subtype M1.

K_i [nM]	M1	M2	M3	M4	M5
Arecoline	19600 ± 2300	2800 ± 700	12700 ± 4500	3600 ± 300	3700 ± 300
DPMARE	3.0 ± 0.5	81.1 ± 29.0	42.6 ± 16.8	12.1 ± 2.9	7.6 ± 0.6
TEGARE	> 4594.6	> 3333.3	> 1666.7	> 2592.6	> 1379.31
DCCARE	> 4594.6	> 3333.3	> 1666.7	> 2592.6	> 1379.31
FDPMARE	4.9 ± 1.6	528.2 ± 85.6	58.7 ± 21.6	14.7 ± 3.7	17.1 ± 2.4
PIROARE	> 4594.6	> 3333.3	> 1666.7	> 2592.6	> 1379.31
PIRNARE	> 4594.6	> 3333.3	> 1666.7	> 2592.6	> 1379.31
NDPMARE	148.1 ± 58.3	3513 ± 127	1136 ± 218	313.8 ± 57.3	307.8 ± 68.4
FEDPMARE	1029 ± 287	3239 ± 868	866.9 ± 278	751.9 ± 432	630.3 ± 115
FDPNMARE	824.9 ± 230	1105 ± 28.0	526.6 ± 129	554.3 ± 330	368.5 ± 34.9
MODPMARE	> 4594.6	> 3333.3	> 1666.7	> 2592.6	> 1379.31
(+)-BrFDPMARE	7.5 ± 1.7	495.8 ± 51.2	39.4 ± 4.5	32.9 ± 1.3	14.5 ± 2.8
(-)-BrFDPMARE	15.1 ± 2.0	414.8 ± 78.5	42.6 ± 7.8	49.8 ± 8.48	22.1 ± 12.2

Table 4-4: K_i values of the tested twelve novel ligands against the mAChR, as well as arecoline as control.

The highest tested concentration for all samples was 1 mM. Some samples, like TEGARE, DCCARE, PIROARE, PIRNARE and MODPMARE, showed a specific signal reduction of less than 50% at the highest tested concentrations of 1 mM, which meant that the K_i could not be calculated. Instead the K_i for the highest concentration (1 mM) was calculated and the conclusion is, that the K_i must be higher than that. Since the K_i value for mAChR tracers should be around 3-50 nM to have sufficient binding affinity for application as PET tracer, higher concentrations were not tested. (Toyohara et al., 2013)

The four structures with the most promising K_i values were DPMARE, FDPMARE and the two enantiomers of BrFDPMARE. All of them even showed a level of subtype selectivity, where they had the highest affinity toward the M1 subtype and M2 seemed to be the least preferred subtype. On a closer look, FDPMARE showed the highest subtype selectivity with a 100 times lower K_i value for M1 than for M2. The two enantiomers of BrFDPMARE differed slightly in the affinity towards different receptors with the highest difference being in the affinity towards M1, where the K_i value of (-)-BrFDPMARE was twice as high. Interestingly, arecoline, the structure on which the ligands are based, shows the highest affinity towards the M2 receptor and the lowest towards the M1. The structures of DPMARE, FDPMARE and BrFDPMARE

are also quite similar with two phenol-rings and in the cases of FDPMARE and BrFDPMARE added halogens. These halogens seem to make an impact on subtype selectivity, as it is higher in the cases of FDPMARE and BrFDPMARE. In the case of MODPMARE it can also be seen, that the replacement of the halogens with methoxy groups decreases the affinity a lot, which could be because of the increased lipophilicity.

Apart from the most promising structures, FEDPMARE and FDPNMARE also showed a subtype selectivity, but they preferred the M5 receptor. Though in FEDPMARE it can be seen, that adding the fluorine group on the other end of the molecule leads to a decrease in affinity. This could be due to the structure of the binding pocket at the receptor. In the case of FDPNMARE, as well as NDPMARE, it can be seen, that the addition of nitrogen in the molecule also doesn't lead to a better affinity.

Last but not least, PIROARE and PIRNARE are probably too large for the binding pocket, resulting again in a low affinity.

4.1.3. Acetylcholinesterase inhibition assay

To be sure, that the assay worked as intended, at first the assay was evaluated using tacrine as positive control. The change in colour intensity from the top left to the bottom right could clearly be seen with this inhibitor of the acetylcholinesterase (Figure 4-7).

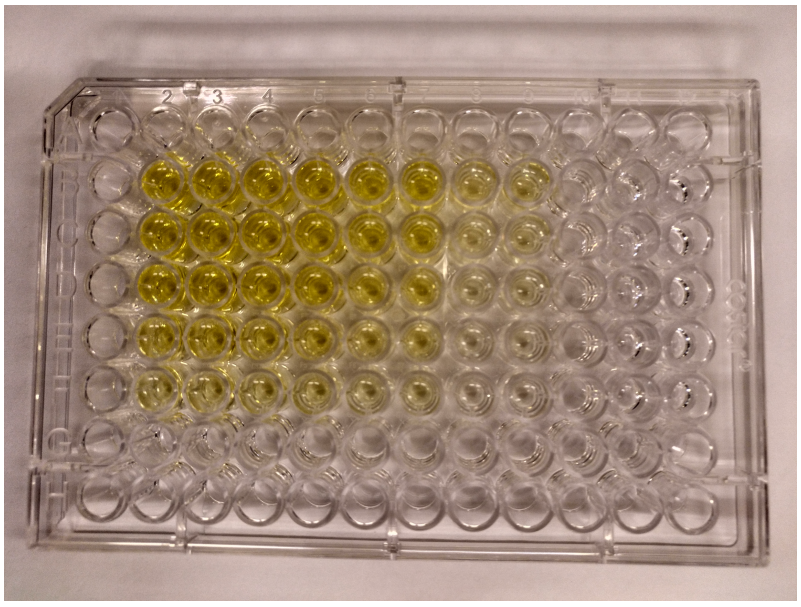

Figure 4-7: 96-well plate used for the Ellman assay of tacrine directly after kinetic measurement.

Therefore, for each concentration, the slope of the kinetic measurement was plotted against the ATI concentration (Figure 4-8).

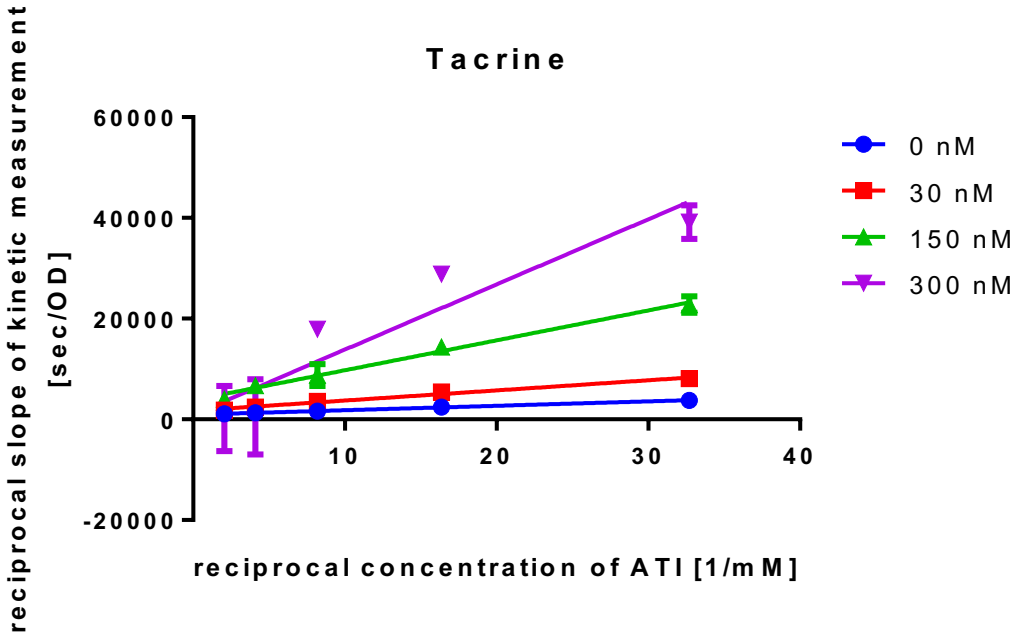

Figure 4-8: Positive control of Ellman assay, using different concentrations of tacrine.

The slopes of each of these lines were then plotted against the concentration of tacrine used (Figure 4-9).

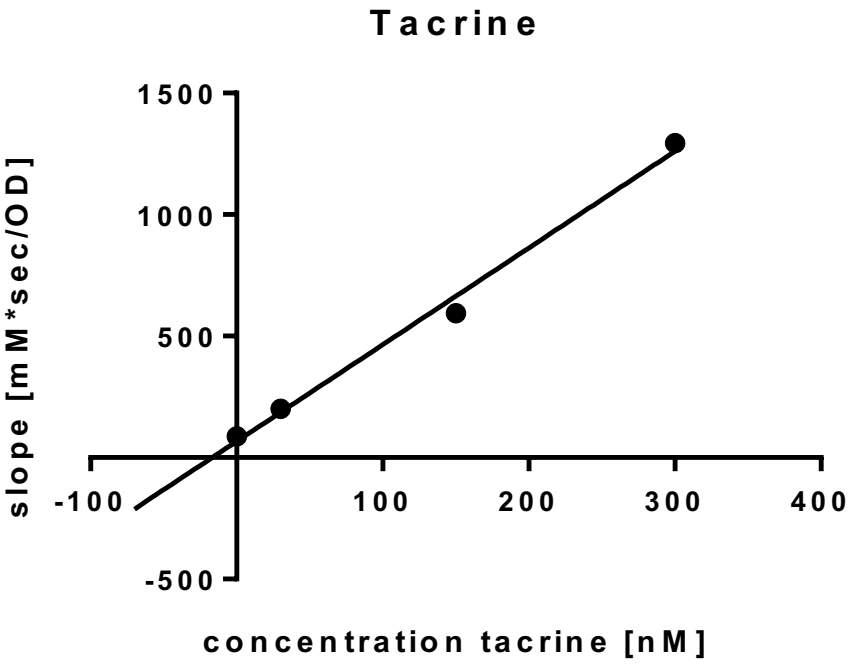

Figure 4-9: Slopes of different ATI concentrations plotted against concentration of tacrine used in the Ellman assay.

In the resulting line the slope equals the k_{on} and the intercept equals the k_{off}. Consequently, the K_i value of tacrine can be calculated using Equation 4-3.

$$K_i = \frac{k_{off}}{k_{on}}$$

Equation 4-3

The determined K_i was 30 +/- 10 nM were in accordance with literature-known K_i-values for tacrine, where the K_i for tacrine against acetylcholinesterase is reported to be between 36 nM and 137 nM. (Darras & Pang, 2017) This proofed that the Ellman assay gives valid results under the used experimental conditions.

For the tested samples, only the highest concentration used in the harvester experiments (1 mM) was measured, which results in a concentration of 16.5 µM used in the assay. Also, in case of BrFDPMARE, only the racemate was tested. Apart from the potential ligands tested in the previous experiments, also pirenzepine was tested. Pirenzepine is a clinically established drug targeting mAChRs. As can be seen in Figure 4-10, Figure 4-11, Figure 4-12 and Figure 4-13 none of the tested substances showed any inhibition of the acetylcholinesterase. The slope remains the same, no matter if a sample is added or simply solvent. To prove that, the slope of each straight was compared with GraphPad Prism 6 via a Dunett's multiple comparison test, using a 2way ANOVA. This test also showed no significant difference between the samples and the blank. Concluding, all tested substances with high affinity to the mAChR show no detectable binding to the off-target acetylcholinesterase at a concentration of 16.5 µM.

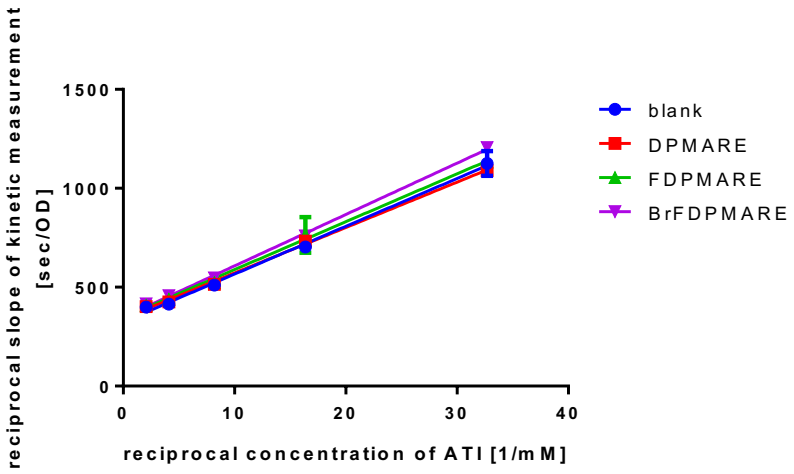

Figure 4-10: Ellman assay result for DPMARE, FDPMARE and BrFDPMARE.

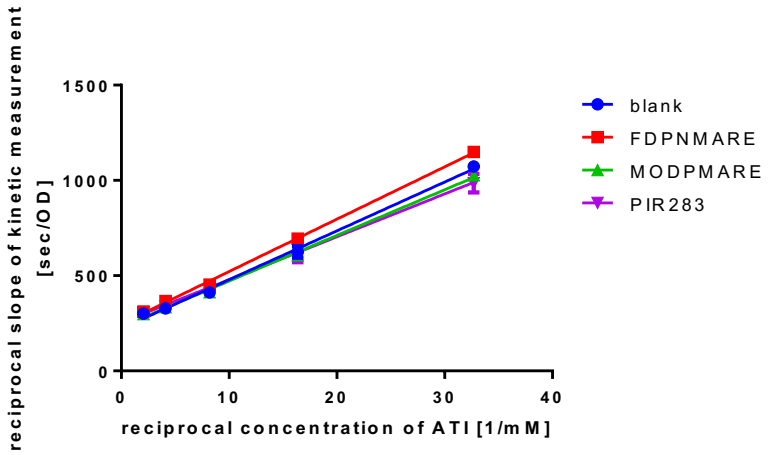

Figure 4-11: Ellman assay result for FDPNMARE, MODPMARE and pirenzepine.

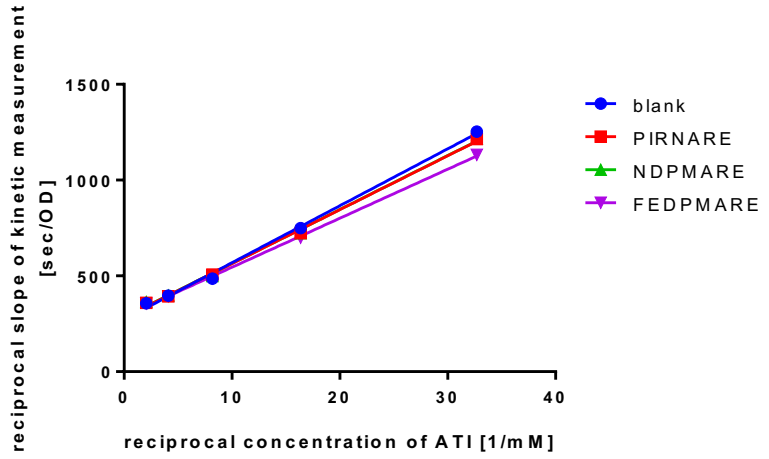

Figure 4-12: Ellman assay result for PIRNARE, NDPMARE and FEDPMARE.

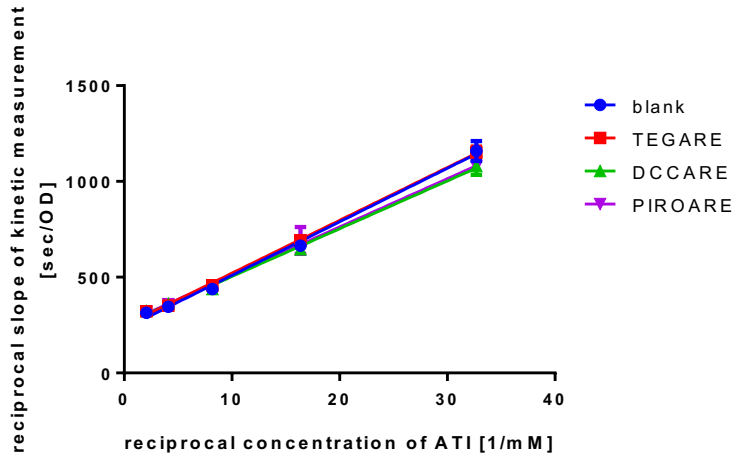

Figure 4-13: Ellman assay result for TEGARE, DCCARE and PIROARE.

4.1.4. Acetylcholinesterase cleavage experiments

Reaction mixtures of the tested compounds and AChE were analysed *via* HPLC to assure that the tested compounds are not prone to AChE cleavage.

For that purpose, at first the chromatograms of the samples with acetylcholinesterase were compared to the chromatograms without acetylcholinesterase. Examples can be seen in Figure 4-14 and Figure 4-15. To prove that no significant hydrolysis occurs under the given condition, a multiple comparisons 2way ANOVA was performed on the areas under the curve of the educt peaks. The only sample which showed a small but significant difference, was the racemic mixture of BrFDPMARE.

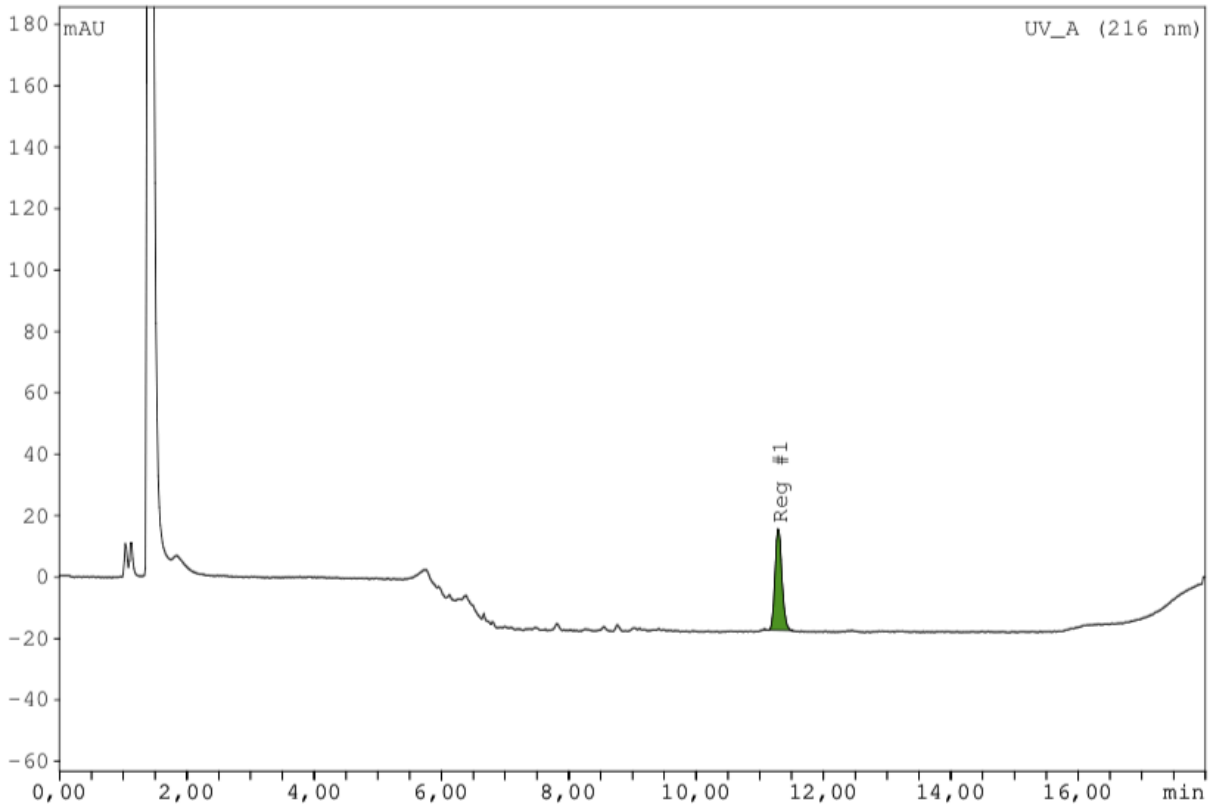

Figure 4-14: HPLC chromatogram of FDPMARE and acetylcholinesterase incubated for 60 minutes.

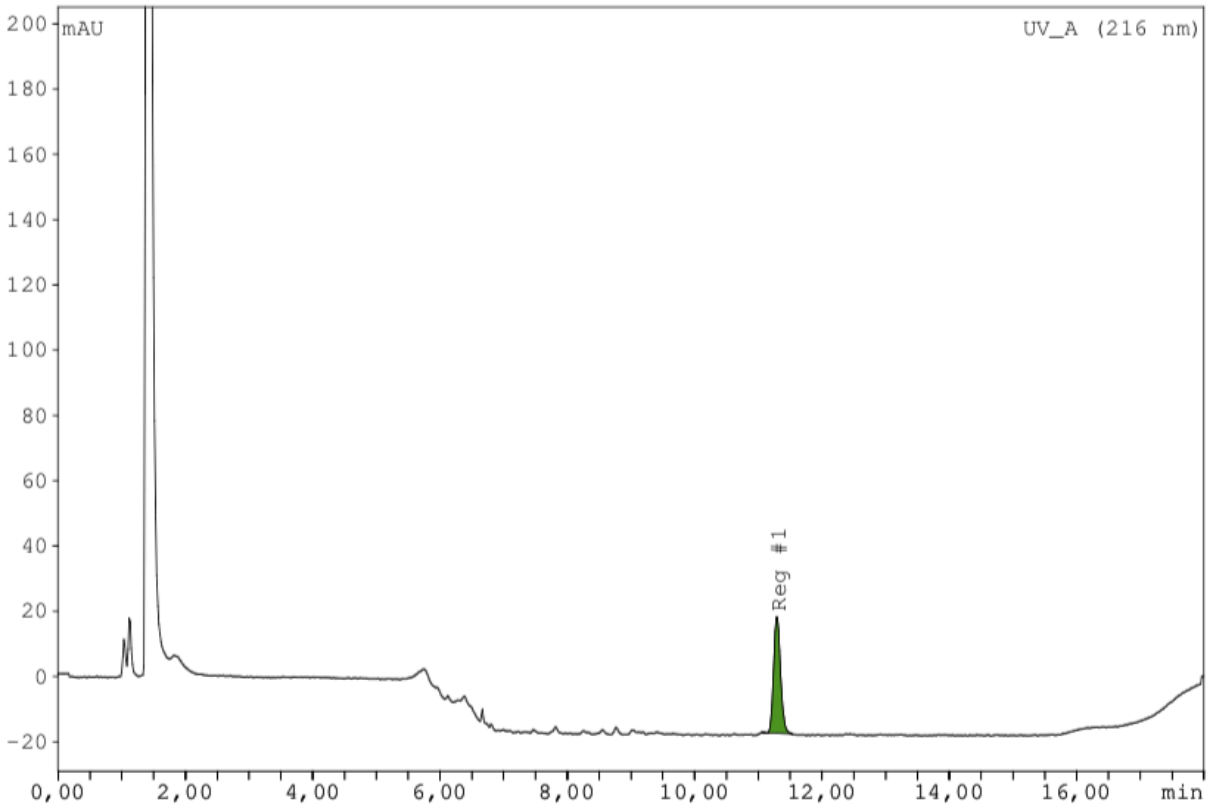

Figure 4-15: HPLC chromatogram of FDPMARE without acetylcholinesterase incubated for 60 minutes.

All the chromatograms were then compared to the chromatogram of arecaidine, which would be the cleaved product (Figure 4-17). Since even in the case of BrFDPMARE, no peak corresponding to the arecaidine peak can be found, it is reasonable to say, that none of the samples are substrates of the acetylcholinesterase.

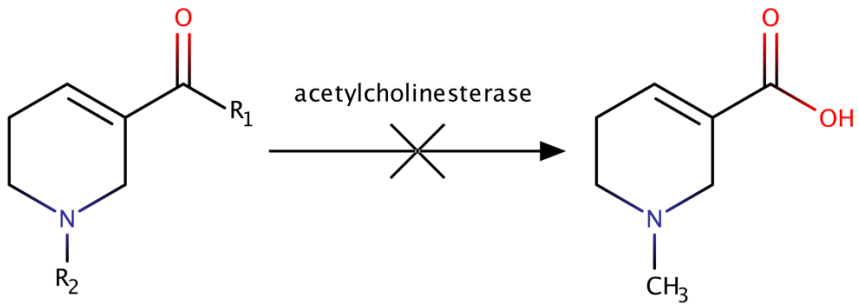

Figure 4-16: Acetylcholinesterase does not cleave arecoline derivatives. For the different residues see Table 4-2.

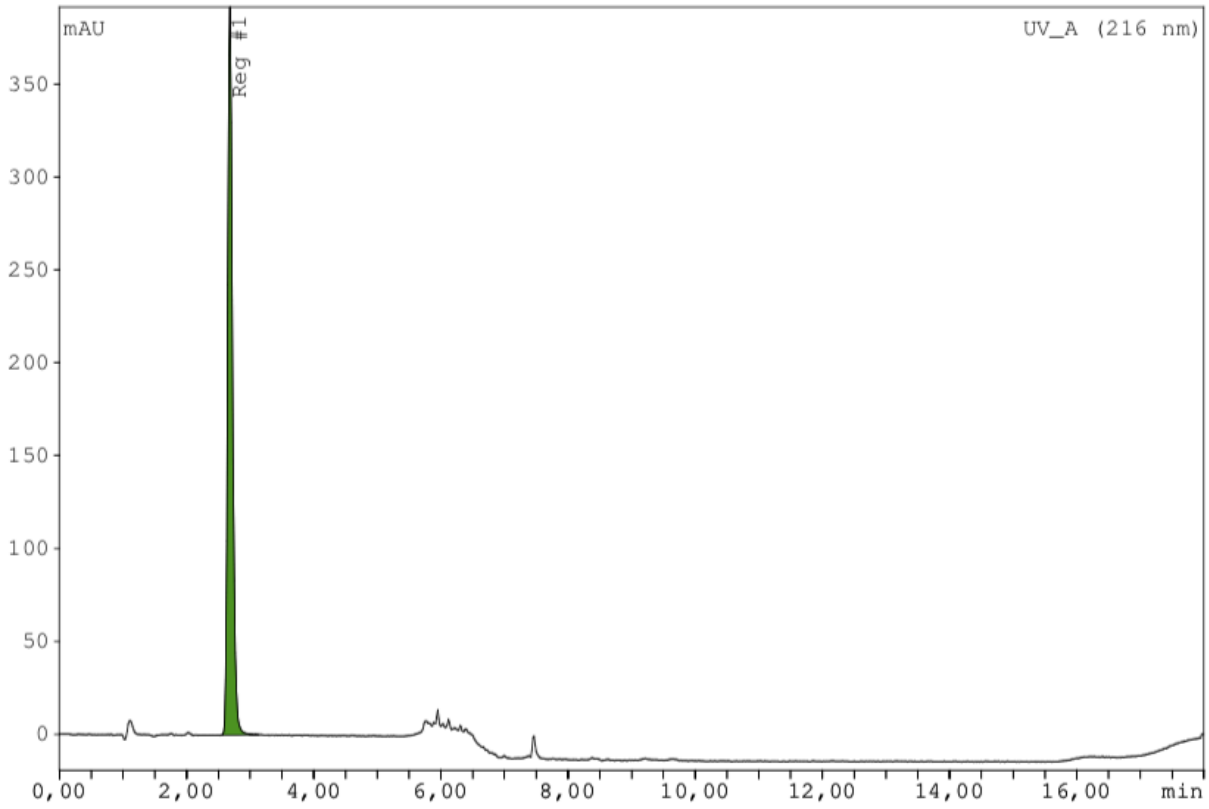

Figure 4-17: HPLC chromatogram of arecaidine.

4.1.5. Ligand Tracer®

Since FDPMARE showed promising binding affinity in the harvester experiments, it was selected for the first few LigandTracer® experiments.

At first, the kinetic behaviour of FDPMARE looked promising. The counts per second increased fast and reached a plateau. The data was later put into GraphPad Prims 6 for further analysis. The curves were fitted using "One-phase association", which uses Equation 4-4 to calculate K_{obs}, the observed rate constant.

$$y = y_0 + (plateau - y_0) * (1 - e^{-K_{obs} * x})$$

Equation 4-4

For this equation y_0 stands for the y-value at the beginning of the experiment, when x=0 and plateau stands for the y-value at infinite times, when the plateau is reached.

After that, the different K_{obs} values were plotted against the concentrations of ^{11}C-labeled FDPMARE used in the experiments. The concentrations were 0.5 nM, 2.5 nM, 5 nM, 10 nM, 25 nM and 50 nM. In theory the correlation should be linear. Then the slope of the line would equal the k_{on} value and the intercept would equal the k_{off} value. In this case the K_i would again

be calculated using Equation 4-5. This relation can be seen in the recent publicaton by Zeilinger, et.al. (Zeilinger et al., 2017)

$$K_i = \frac{k_{off}}{k_{on}}$$

Equation 4-5

As can be seen in (Figure 4-18) there was a trend for increasing K_{obs} but the correlation for [^{11}C]FDPMARE was not strictly linear.

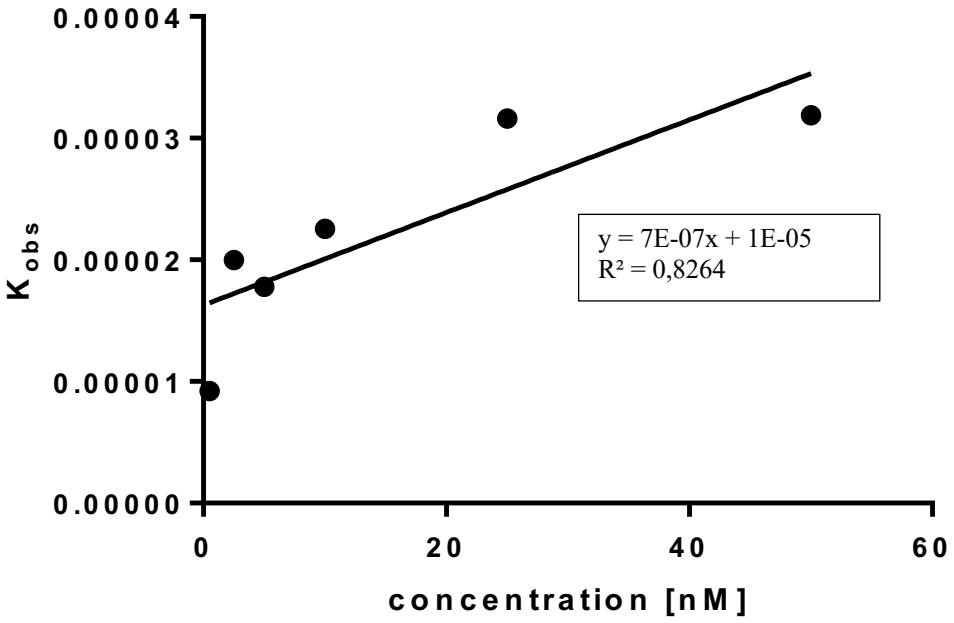

Figure 4-18: K_{obs} plotted against the concentrations of [^{11}C]FDPMARE.

In order to understand why the correlation was not strictly linear, a comparison of the normalized curves was done, see Figure 4-19.

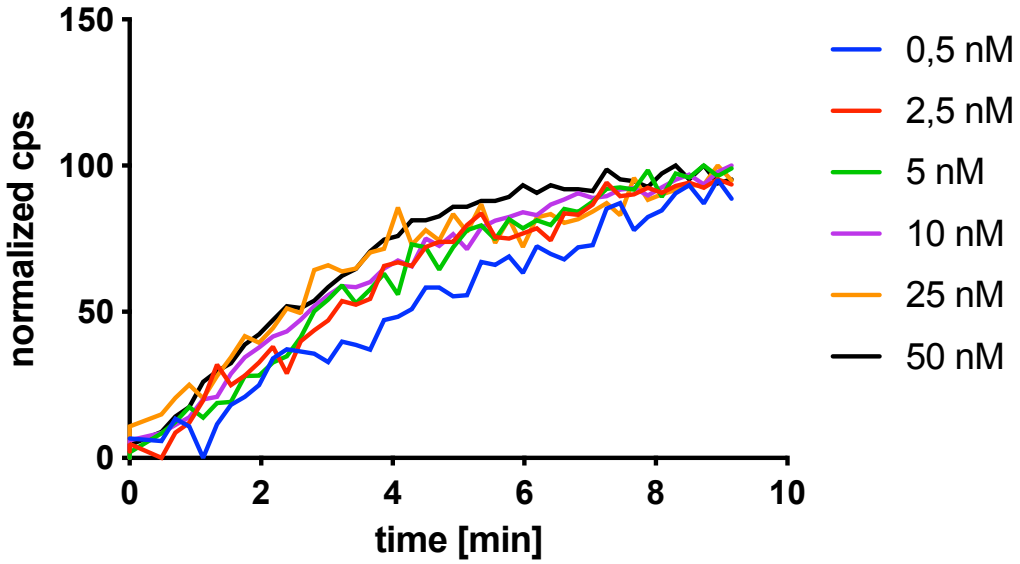

Figure 4-19: LigandTracer® experiment with different concentrations of [^{11}C]FDPMARE and CHO cells stably transfected with mAChR M1.

In the case of specific binding, the steepness of the curves should change corresponding to the concentration of radioligand used. An assumption for this not expected behaviour is the potential unspecific binding of FDPMARE. Another potential explanation is that the ligand is not only binding to the receptor but is further internalized and accumulated. Consequently, not only the process of the binding kinetic is described by the experiment, but it also involves further processes which cannot be described independently.

In the next step DPMARE was used, as it had the second-best affinity towards mAChR. To further prove the problem of unspecific binding, four different concentrations of [^{11}C]DPMARE (0.3 nM, 3 nM, 10 nM, 30 nM) were added to the same petri dish consecutively, after the signal had reached a plateau. In parallel a second petri dish was pre-blocked with scopolamine (10 µM). Since scopolamine has a high affinity of 1.3 nM to mAChR's (Toyohara et al., 2013), there should be very little to no binding on the second petri dish, if the binding was specific. Afterwards, again the curves provided by the LigandTracer® Control software, were normalized using GraphPad Prism 6 and put above each other (Figure 4-20).

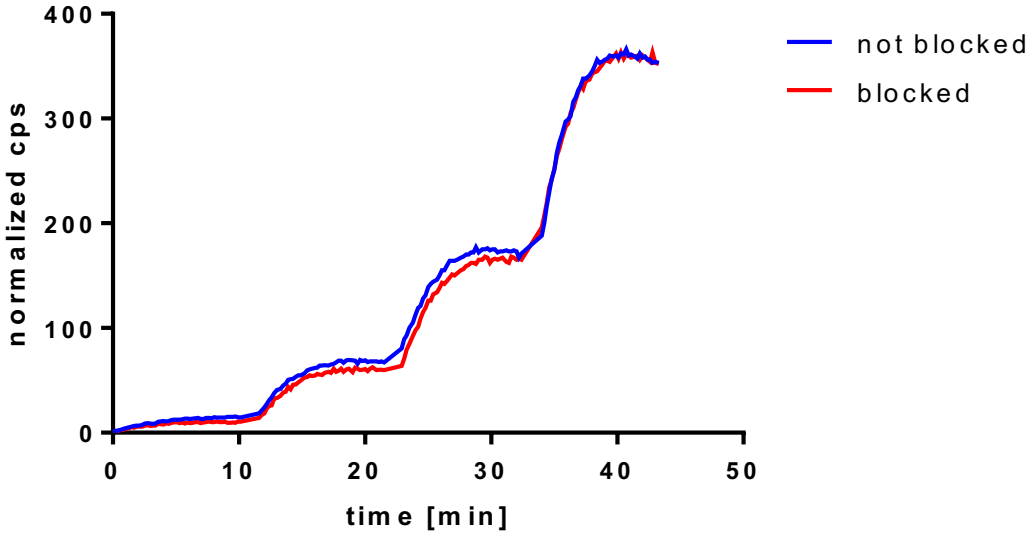

Figure 4-20: LigandTracer® experiment using [^{11}C]DPMARE and CHO cells stably transfected with mAChR M1.

As can be seen in Figure 4-20, the curve remained the same, even though one petri dish was pre-blocked with scopolamine.

The experiment was repeated using [^{11}C]pirenzepine. Pirenzepine is already used as a drug targeting the mAChR. (Drugbank, 2019) This experiment should prove that the setup of the LigandTracer® experiment works. Again, one petri dish was pre-blocked using scopolamine (10 µM), while the other one was not blocked. The concentrations of [^{11}C]pirenzepine used were 0.5 nM, 1 nM, 10 nM and 100 nM. The resulting data was normalized with GraphPad Prism 6 and the curves where put on top of each other (Figure 4-21).

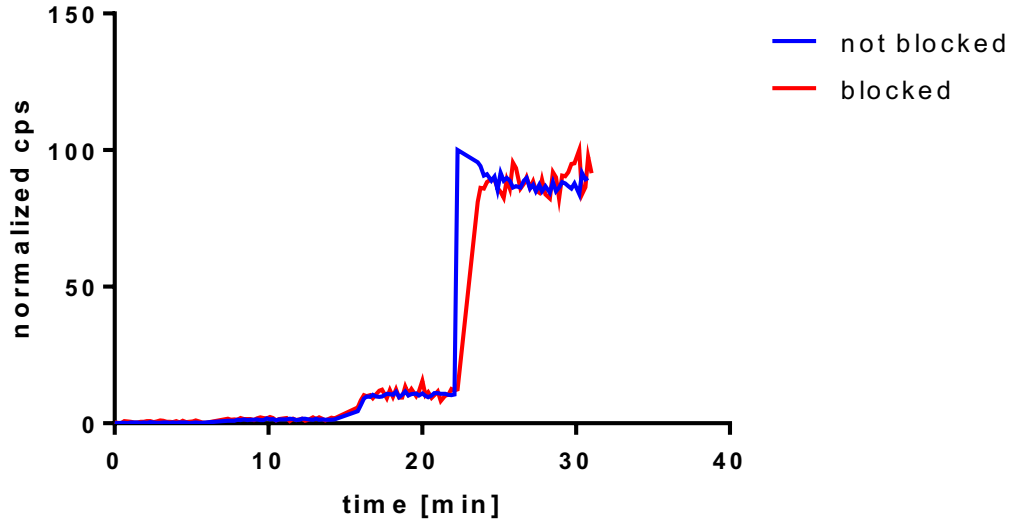

Figure 4-21: LigandTracer® experiment using [^{11}C]pirenzepine and CHO cells stably transfected with mAChR M1.

As can be seen in Figure 4-21, both curves had a nearly similar course. As pirenzepine is a well-known mAChR ligand, which specifically binds to the mAChR, it is likely that there is a methodological problem behind these unexpected results.
Therefore, it was tested, if the setup of the LigandTracer® experiment may be at fault. For this purpose, cells were cultivated in petri dishes in the same way, as for the other LigandTracer® experiments. Then the petri dishes were put on the LigandTracer® and the medium was changed. The petri dishes were left to rotate and later a picture of the cells was taken (Figure 4-22).

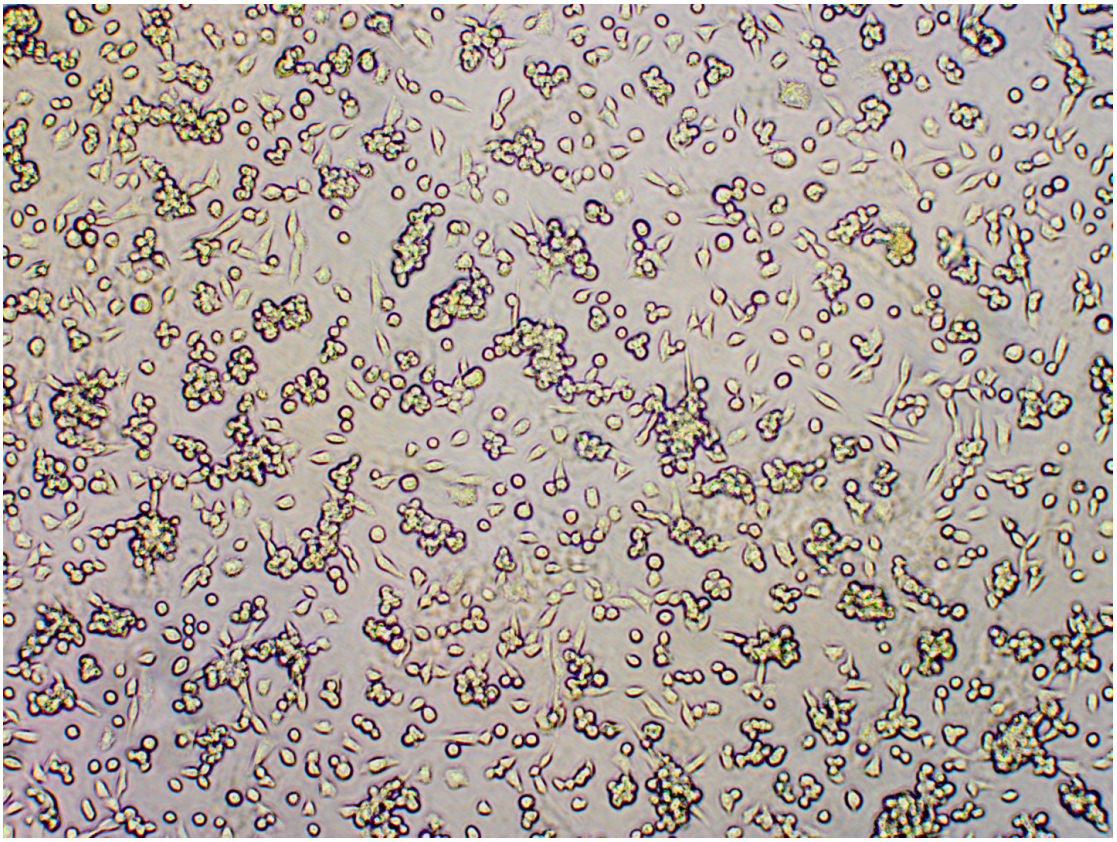

Figure 4-22: CHO cells after rotating on the LigandTracer®.

In Figure 4-22 it can be seen that the cells look healthy. Most of the cells still have an elongated, rhomboid form. When cells die, they detach from the bottom of the flask or petri dish, in which they are cultivated, and become round. This only happened to some of the cells in Figure 4-22. Since the rotation was not responsible for the unusual results of the experiments, the next step was to see how the cells reacted to the added radiotracer. Since in this case the binding was not measured, cold pirenzepine was used. To mimic the composition of the tracer solution used in previous experiments, 15 mL of NaCl, 6 mL of PET-PPP-buffer, 1.5 mL of ethanol and 1.55 µL of pirenzepine (0.9 mg/mL) were combined in a falcon tube. 500 µL of this solution were added

to the cells in the petri dish, which had been put onto the LigandTracer®. The cells were left to rotate and after an hour another picture was taken (Figure 4-23).

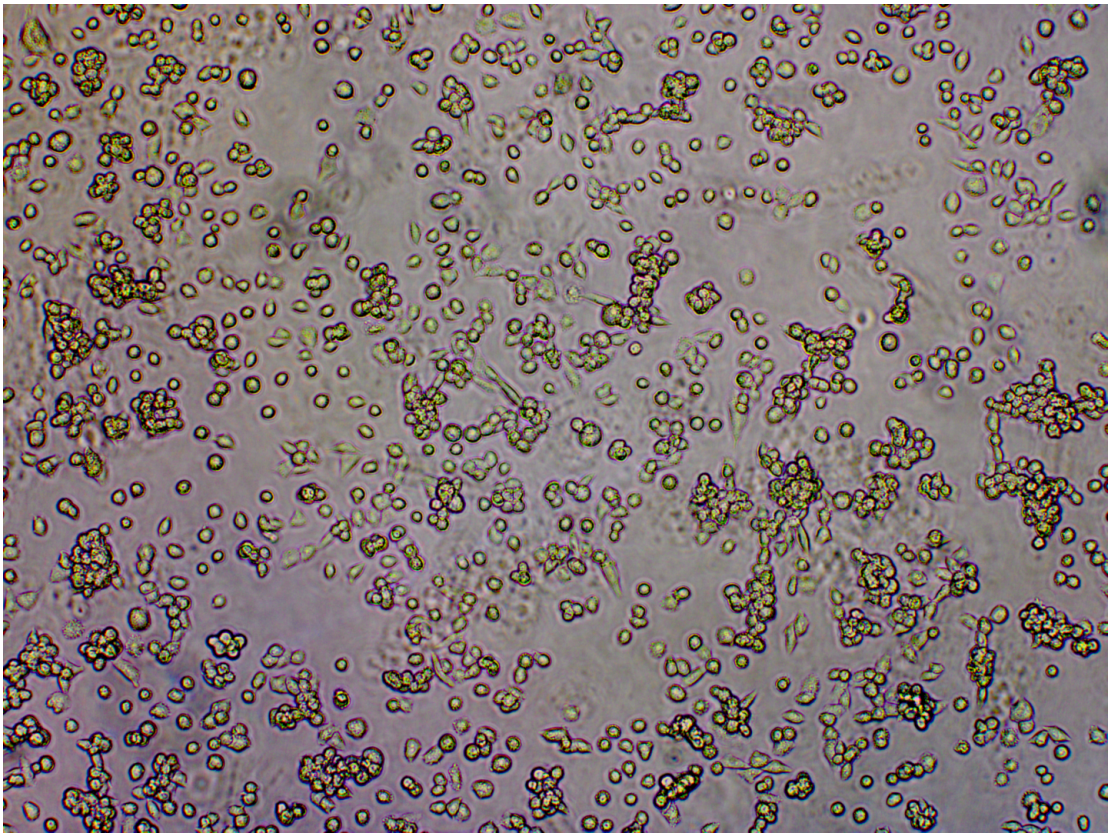

Figure 4-23: CHO cells after the addition of the cold tracer-solution and after rotating on the LigandTracer®.

As can be seen in Figure 4-23, in this case nearly all of the cells are round, which means, they all got detached from the bottom of the petri dish. This in turn means, that the cells cannot survive in the conditions used for the LigandTracer® experiment. On the one hand, this could be due to the pirenzepine in the solution, though this is not very likely as pirenzepine is an already approved drug and should not damage the cells that much. On the other hand, this could be due to the amount of ethanol in the solution. This is more likely, as ethanol is toxic for the cells in too high concentrations. Though the concentration used in this experiment should still be too little for the damage that is done to the cells. Also, this explains the results of the experiments with pirenzepine. Since the cells detach from the bottom of the petri dish, the detector of the LigandTracer® never actually measures the binding to the cells.
However, further experiments are necessary to prove if specific binding, internalization or off-target binding, causes the results or if the methodology has to be changed.

5. Conclusion and outlook

Towards the identification of potential new ligands for the mAChR twelve derivatives of arecoline were tested for their affinity to all five subtypes of the mAChR.

All things considered, out of the twelve arecoline derivatives seven had K_i values in micro- to nanomolar range. Out of those seven, four showed very promising K_i as well as high subtype selectivity for the M1. This would be an added bonus for a new PET tracer for the mAChR, as most of the already established ones don't show a subtype selectivity.

None of the tested derivatives of arecoline proofed to be an inhibitor or a substrate to the off-target acetylcholinesterase. Since any kind of binding to an off-target, like acetylcholinesterase, could interfere with the imaging of the desired binding to the acetylcholine receptors, these results show that in theory the tested structures would be ideal for PET-imaging as they have a high specificity for the target. This combined with the found K_i values lead to the four structures which were applied to further testing, namely FDPMARE, DPMARE and the two enantiomers of BrFDPMARE.

The results of the LigandTracer® experiments were not as expected, which was probably due to the binding being mostly unspecific, high accumulation of the substances or a low expression of the receptor expressed on the cells. Still, there is also the possibility that the setup of the experiment was not ideal for the CHO cells used. It is possible that a change in setup would show more specific binding. Therefore, the setup of the LigandTracer® experiments needs to be revaluated.

However, the next steps would be to identify less lipophilic structures, with similar or better mAChR selectivity and specificity. These could be screened again for their K_i values and would maybe show less unspecific binding.

6. Bibliography

Bailey, D. L., Townsend, D. W., Valk, P. E., & Maisey, M. N. (2005). *Positron emission tomography*. *Molecular Imaging Techniques: New Frontiers*. https://doi.org/10.4155/EBO.12.504

Cheng, Y.-C., & Prusoff, W. H. (1973). Relationship Between Inhibition Constant and IC50. *Biochemical Pharmacology*, *22*, 3099–3108.

Darras, F. H., & Pang, Y. P. (2017). On the use of the experimentally determined enzyme inhibition constant as a measure of absolute binding affinity. *Biochemical and Biophysical Research Communications*, *489*(4), 451–454. https://doi.org/10.1016/j.bbrc.2017.05.168

Davenport, A. P., & Russell, F. D. (2011). Radioligand Binding Assays: Theory and Practice. *Current Directions in Radiopharmaceutical Research and Development*, 169–179. https://doi.org/10.1007/978-94-009-1768-2_11

Dong, G. Z., Kameyama, K., Rinken, A., & Haga, T. (1995). Ligand binding properties of muscarinic acetylcholine receptor subtypes (m1-m5) expressed in baculovirus-infected insect cells. *Journal of Pharmacology and Experimental Therapeutics*, *274*(1), 378–384.

Drugbank. (2019). Pirenzepine. Retrieved May 16, 2019, from https://www.drugbank.ca/drugs/DB00670

Eglen, R. M., Choppin, A., & Watson, N. (2001). Therapeutic opportunities from muscarinic receptor research. *Trends in Pharmacological Sciences*, *22*(8), 409–414. https://doi.org/10.1016/S0165-6147(00)01737-5

Ellman, G. L. (1959). Tissue Sulfhydryl Groups. *American Journal of Analytical Chemistry*, 70–77.

Heilbronn, E., & Bartfai, T. (1978). Muscarinic acetylcholine receptor. *Progress in Neurobiology*, *11*, 171–188.

Ishii, M., & Kurachi, Y. (2006). Muscarinic Acetylcholine Receptors. *Current Pharmaceutical Design*, *12*, 3573–3581. https://doi.org/10.1007/978-1-4419-6247-8_14273

Keen, M., & Qume, M. (2003). Overview of Ligand-Receptor Binding Techniques. *Receptor Binding Techniques*, *106*, 3–23. https://doi.org/10.1385/0-89603-530-1:3

Koeppe, R. A., Frey, K. A., Mulholland, G. K., Kilbourn, M. R., Buck, A., Lee, K. S., & Kuhl, D. E. (1994). [11C]tropanyl benzilate-binding to muscarinic cholinergic receptors: Methodology and kinetic modeling alternatives. *Journal of Cerebral Blood Flow and Metabolism*, *14*(1), 85–99. https://doi.org/10.1038/jcbfm.1994.13

Kruse, A. C., Kobilka, B. K., Gautam, D., Sexton, P. M., Christopoulos, A., & Wess, J. (2014). Muscarinic acetylcholine receptors: Novel opportunities for drug development. *Nature Reviews Drug Discovery*, *13*(7), 549–560. https://doi.org/10.1038/nrd4295

Kumar, A., & Darreh-Shori, T. (2017). DMSO: A Mixed-Competitive Inhibitor of Human Acetylcholinesterase. *ACS Chemical Neuroscience*, *8*(12), 2618–2625. https://doi.org/10.1021/acschemneuro.7b00344

Liu, Y. J., Peng, W., Hu, M. B., Xu, M., & Wu, C. J. (2016). The pharmacology, toxicology and potential applications of arecoline: a review. *Pharmaceutical Biology*, *54*(11), 2753–2760. https://doi.org/10.3109/13880209.2016.1160251

McPherson, D. W. (2001). Receptors with Radioligands for Diagnostic Nuclear Medicine Studies. *Ion Channel Localization*, 17–38.

Missouri University of Science & Technology. (2010a). Stable Transfected Cell Line (CHO-K1) M1 Muscarinic Receptor (human), wild-type QA & Additional Information.

Missouri University of Science & Technology. (2010b). Stable Transfected Cell Line (CHO-K1) M2 Muscarinic Receptor (human), wild-type QA & Additional Information.

Missouri University of Science & Technology. (2010c). Stable Transfected Cell Line (CHO-K1) M3 Muscarinic Receptor (human), wild-type QA & Additional Information.

Missouri University of Science & Technology. (2010d). Stable Transfected Cell Line (CHO-K1) M4 Muscarinic Receptor (human), wild-type QA & Additional Information.

Missouri University of Science & Technology. (2010e). Stable Transfected Cell Line (CHO-K1) M5 Muscarinic Receptor (human), wild-type QA & Additional Information.

Motulsky, H., & Neubig, R. (2002). Analyzing radioligand binding data. *Current Protocols in Neuroscience*, *Chapter 7*, Unit 7.5. https://doi.org/10.1002/0471142301.ns0705s19

PerkinElmer. (2009a). Human Muscarinic Acetylcholine Receptor M 1 Cell Line.

PerkinElmer. (2009b). Human Muscarinic Acetylcholine Receptor M 2 Cell Line.

PerkinElmer. (2009c). Human Muscarinic Acetylcholine Receptor M 3 Cell Line.

PerkinElmer. (2009d). Human Muscarinic Acetylcholine Receptor M 4 Cell Line.

PerkinElmer. (2009e). Human Muscarinic Acetylcholine Receptor M 5 Cell Line.

Pike, V. W. (2009). PET radiotracers: crossing the blood-brain barrier and surviving metabolism. *Trends in Pharmacological Sciences*, *30*(8), 431–440. https://doi.org/10.1016/j.tips.2009.05.005.PET

Ridgeview. (2019). Understanding how your ligand interacts with living cells. Retrieved May 16, 2019, from http://www.ligandtracer.com/docs/LigandTracer Technology Note 1.6.pdf

Thermo Fisher Scientific. (2011). User Guide: Pierce BCA Protein Assay Kit. *Pierce Biotechnology*. https://doi.org/10.1016/j.ijproman.2010.02.012

Toyohara, J., Sakata, M., & Ishiwata, K. (2013). *Human Brain Imaging of Acetylcholine Receptors*. *Imaging of the Human Brain in Health and Disease*. Elsevier. https://doi.org/10.1016/B978-0-12-418677-4.00007-5

Worek, F., Eyer, P., & Thiermann, H. (2012). Determination of acetylcholinesterase activity by the Ellman assay: A versatile tool for in vitro research on medical countermeasures against organophosphate poisoning. *Drug Testing and Analysis*, *4*(3–4), 282–291. https://doi.org/10.1002/dta.337

Zeilinger, M., Pichler, F., Nics, L., Wadsak, W., Spreitzer, H., Hacker, M., & Mitterhauser, M. (2017). New approaches for the reliable in vitro assessment of binding affinity based on high-resolution real-time data acquisition of radioligand-receptor binding kinetics. *EJNMMI Research*, *7*(1). https://doi.org/10.1186/s13550-016-0249-9

List of figures

List of tables